

1 **Impacts of biogenic polyunsaturated aldehydes on metabolism and community**  
2 **composition of particle-attached bacteria in coastal hypoxia**

3 Zhengchao Wu<sup>1,2</sup>, Qian P. Li<sup>1,2,3,\*</sup>, Zaiming Ge<sup>1,3</sup>, Bangqin Huang<sup>4</sup>, Chunming Dong<sup>5</sup>

4 <sup>1</sup>State Key Laboratory of Tropical Oceanography, South China Sea Institute of Oceanology, Chinese  
5 Academy of Sciences, Guangzhou, China

6 <sup>2</sup>Southern Marine Science and Engineering Guangdong Laboratory, Guangzhou, China

7 <sup>3</sup>College of Marine Science, University of the Chinese Academy of Sciences, Beijing, China

8 <sup>4</sup>Fujian Provincial Key Laboratory of Coastal Ecology and Environmental Studies, State Key Laboratory of  
9 Marine Environmental Science, Xiamen University, Xiamen, China

10 <sup>5</sup>Key Laboratory of Marine Genetic Resources, Third Institute of Oceanography, MNR, Xiamen, China

11 \*Correspondence to: Qian Li (qianli@scsio.ac.cn)

12

13 **Abstract.** Eutrophication-driven coastal hypoxia is of great interest for decades, though its mechanisms  
14 remain not fully understood. Here, we showed elevated concentrations of particulate and dissolved  
15 polyunsaturated aldehydes (PUAs) associated with the hypoxic waters in the bottom layer of a salt-wedge  
16 estuary. Bacterial respiration within the hypoxic waters was mainly contributed by particle-attached  
17 bacteria (PAB) (>0.8  $\mu\text{m}$ ), with free-living bacteria (0.2-0.8  $\mu\text{m}$ ) only accounting for 25-30 % of the total  
18 rate. The concentration of particle-adsorbed PUAs ( $\sim 10 \mu\text{mol L}^{-1}$ ) in the hypoxic waters were directly  
19 quantified for the first time based on large-volume-filtration and subsequent on-site PUAs derivation and  
20 extraction. PUAs-amended incubation experiments for PAB (>25  $\mu\text{m}$ ) associated with sinking or suspended  
21 particles retrieved from the low-oxygen waters were also performed to explore the impacts of PUAs on the  
22 growth and metabolism of PAB and associated oxygen utilization. We found an increase in cell growth of  
23 PAB in response to low-dose PUAs ( $1 \mu\text{mol L}^{-1}$ ) but an enhanced cell-specific bacterial respiration and  
24 production in response to high-dose PUAs ( $100 \mu\text{mol L}^{-1}$ ). Improved cell-specific metabolism of PAB in

25 response to high-dose PUAs was also accompanied by a shift of PAB community structure with increased  
26 dominance of genus *Alteromonas* within the Gammaproteobacteria. We thus conclude that a high PUAs  
27 concentration associated with aggregate particles within the bottom layer may be crucial for some species  
28 within *Alteromonas* to regulate PAB community structure. The change of bacteria community could lead to  
29 an enhancement of oxygen utilization during the degradation of particulate organic matters and thus likely  
30 contribute to the formation of coastal hypoxia. These findings are potentially important for coastal systems  
31 with large river inputs, intense phytoplankton blooms driven by eutrophication, as well as strong hypoxia  
32 developed below the salt-wedge front.

## 33 **1. Introduction**

34 Coastal hypoxia, defined as dissolved oxygen levels  $< 62.5 \mu\text{mol kg}^{-1}$ , has become a worldwide problem in  
35 recent decades (Diaz and Rosenberg, 2008; Helm et al., 2011). It could affect diverse life processes from  
36 genes to ecosystems, resulting in the spatial and temporal change of marine food-web structures (Breitburg  
37 et al., 2018). Coastal deoxygenation is also tightly coupled with other global issues, such as global warming  
38 and ocean acidification (Doney et al., 2012). Formation and maintenance of eutrophication-derived hypoxia  
39 in the coastal waters should reflect the interaction between physical and biogeochemical processes (Kemp  
40 et al., 2009). Generally, seasonal hypoxia occurs in the coastal ocean when strong oxygen sinks are coupled  
41 with restricted resupply during periods of strong density stratification. Termination of the event occurs with  
42 oxygen resupply when stratification is eroded by vertical mixing (Fennel and Testa, 2019).

43 Bacterial respiration accounts for the largest portion of aquatic oxygen consumption and is thus pivotal  
44 for the development of hypoxia and oxygen minimum zones (Williams and del Giorgio, 2005; Diaz and  
45 Rosenberg, 2008). Generally, free-living bacteria (FLB,  $0.2\text{-}0.8 \mu\text{m}$ ) dominate the community respiration in  
46 many parts of the ocean (Robinson and Williams, 2005; Kirchman, 2008). Compared to the FLB, the role  
47 of particle-attached bacteria (PAB,  $>0.8 \mu\text{m}$ ) on community respiration is less addressed, particularly in the  
48 coastal oceans. In some coastal waters, PAB can be more important than the FLB with a higher metabolic  
49 activity that might affect carbon cycle through organic matter remineralization (Garneau et al., 2009; Lee et  
50 al., 2015). PAB was found more abundant than the FLB with a higher diversity near the mouth of the Pearl  
51 River estuary (PRE) (Li et al., 2018; Liu et al., 2020; Zhang et al., 2016). An increased contribution of PAB  
52 to respiration relative to FLB can occur during the development of coastal phytoplankton bloom (Huang et  
53 al., 2018). In the Columbia River estuary, the particle-attached bacterial activity could be 10-100 folds  
54 higher than that of its free-living counterparts leading to its dominant role in organic detritus  
55 remineralization (Crump et al., 1998). Therefore, it is crucial to assess the respiration process associated  
56 with PAB and its controlling factors in these regions, to fully understand oxygen utilization in the hypoxic  
57 area with an intense supply of particulate organic matters.

58        There is an increasing area of seasonal hypoxia in the nearshore bottom waters of the Pearl River  
59 Estuary and the adjacent northern South China Sea (NSCS) (Yin et al., 2004; Zhang and Li 2010; Su et al.,  
60 2017). The hypoxia is generally developed at the bottom of the salt-wedge where downward mixing of  
61 oxygen is restrained due to increased stratification and where there is an accumulation of  
62 eutrophication-derived organic matter due to flow convergence driven by local hydrodynamics (Lu et al.,  
63 2018). Besides physical and biogeochemical conditions, aerobic respiration is believed the ultimate cause  
64 of hypoxia here (Su et al., 2017). Thus, microbial respiration had been strongly related to the consumption  
65 of bulk dissolved organic carbon in the PRE hypoxia (He et al., 2014).

66        Phytoplankton-derived polyunsaturated aldehydes (PUAs) are known to affect marine microorganisms  
67 over various trophic levels by acting as infochemicals and/or by chemical defenses, which strengthen their  
68 potential importance in natural environments (Ribalet et al., 2008; Ianora and Miralto, 2010; Edwards et al.,  
69 2015; Franzè et al., 2018). PUAs are produced by stressed diatoms during the oxidation of membrane  
70 polyunsaturated fatty acids (PUFA) by lipoxygenase (Pohnert 2000) and are released from the surface of  
71 particles to the seawater by diffusion. A perennial bloom of PUA-producing diatoms near the mouth of the  
72 PRE (Wu and Li, 2016) should support the importance of PUAs relative to other phytoplankton-derived  
73 organic compounds, such as karlotoxin by dinoflagellates, cyanotoxin by cyanobacteria, and  
74 dimethylsulphonioacetate mainly by prymnesiophytes. Besides PUAs, there are other signaling  
75 molecules that may potentially affect bacterial activities in the low oxygen waters, such as  
76 2-n-pentyl-4-quinolinol (PQ) and acylated homoserine lactones (AHL). PQ could be less important here in  
77 terms of hypoxia formation as it is generally produced as antibiosis by PAB such as *Alteromonas sp.* to  
78 inhibit respirations of other PAB (Long et al., 2003). AHL could also play a less important role here since  
79 the AHL-mediated quorum-sensing could be constrained by a large pH fluctuation from 7.2 to 8.8 in the  
80 bottom waters of the PRE (Decho et al., 2009).

81        The level of PUAs in the water-column are inhomogeneous, varying from sub-nanomolar offshore to  
82 nanomolar nearshore (Vidoudez et al., 2011; Wu and Li, 2016; Bartual et al., 2018), and to micromolar

83 associated with particle hotspots (Edwards et al., 2015). The strong effect of PUAs on bacterial growth,  
84 production, and respiration has been well demonstrated in laboratory studies (Ribalet et al., 2008) and field  
85 studies (Balestra et al., 2011; Edwards et al., 2015). A nanomolar level of PUAs recently reported in the  
86 coastal waters outside the PRE was hypothesized to affect oxygen depletion by promoting microbial  
87 utilization of organic matters in the bottom waters (Wu and Li, 2016). Meanwhile, the actual role of PUAs  
88 on bacterial metabolism within the bottom hypoxia remains largely unexplored.

89 In this study, we investigate the particle-attached bacteria within the core of the hypoxic waters by  
90 exploring the linkage between PUAs and bacterial oxygen utilization on the suspended organic particles.  
91 There are three specific questions to address here: What are the relative roles of PAB and FLB on bacterial  
92 respiration in the hypoxic waters? What are the actual levels of PUAs in the hypoxic waters? What are the  
93 responses of PAB to PUAs in the hypoxic waters? For the first question, size-fractionated bacterial  
94 respiration rates were estimated for both FLB (0.2-0.8  $\mu\text{m}$ ) and PAB (>0.8  $\mu\text{m}$ ) in the hypoxic waters. For  
95 the second question, the concentrations of particulate and dissolved PUAs within the hypoxic waters were  
96 measured in the field. Besides, the hotspot PUAs concentration associated with the suspended particles  
97 within the hypoxic waters was directly quantified for the first time using large-volume filtration and  
98 subsequent on-site derivation and extraction. For the third question, field PUAs-amended incubation  
99 experiments were conducted for PAB (>25  $\mu\text{m}$ ) retrieved from the low-oxygen waters. We focused on  
100 particles of >25  $\mu\text{m}$  to explore the role of PUAs on PAB associated with sinking aggregates and large  
101 suspended particles (it may not be directly comparable to other size cut-offs in the literature). The doses of  
102 PUAs treatments were selected to represent the actual levels of PUAs hotspots, to assess the PAB responses  
103 (including bacterial abundance, respiration, production, and community composition) to the exogenous  
104 PUAs in the hypoxic waters. By synthesizing these experimental results with the change of water-column  
105 biogeochemistry, we hope to explore the underlying mechanism for particle-adsorbed PUAs influencing on  
106 community structure and metabolism of PAB in the low-oxygen waters, as well as to understand its  
107 contribution to coastal deoxygenation of the NSCS shelf-sea.

108

## 109 **2. Methods**

### 110 **2.1 Descriptions of field campaigns and sampling approaches**

111 Field survey cruises were conducted in the PRE and the adjacent NSCS during June 17<sup>th</sup>-28<sup>th</sup>, 2016 and  
112 June 18<sup>st</sup>-July 2<sup>nd</sup>, 2019 (Figure 1). Briefly, vertical profiles of temperature, salinity, dissolved oxygen, and  
113 turbidity were acquired from a Seabird 911 rosette sampling system. The oxygen sensor data were corrected  
114 by field titration measurements during the cruise. Water samples at various depths were collected using 6 or  
115 12 liters (12 or 24 positions) Niskin bottles attached to the Rosette sampler. Surface water samples were  
116 collected at ~1m or 5 m depth, while bottom water samples were obtained at depths ~4 m above the bottom.  
117 Chlorophyll-*a* (Chl-*a*) samples were taken at all depths at all stations and nutrients were also sampled  
118 except at a few discrete stations. For the 2016 cruise, samples for pPUAs were collected at all depths close  
119 to station X1 (Figure 1A). During the summer of 2019, vertical profiles of particulate PUAs (pPUAs) and  
120 dissolved PUAs (dPUAs) were determined at Y1 in the hypoxic zone and Y2 outside the hypoxic zone with  
121 field PUAs-amended experiments conducted at Y1 (Figure 1B). For station Y1, the middle layer was  
122 defined as 12 m with the bottom layer as 25 m. At this station, samples at different depths were collected  
123 for determining the size-fractionated respiration rates and the whole water bacterial taxonomy.

124

### 125 **2.2 Determination of chlorophyll-*a*, dissolved nutrients**

126 For Chl-*a* analyses, 500 mL of water sample was gently filtered through a 0.7  $\mu\text{m}$  Whatman GF/F filter.  
127 The filter was then wrapped by a piece of aluminum foil and stored at -20 °C on board. Chl-*a* was extracted  
128 at 4 °C in the dark for 24 h using 5 mL of 90% acetone. After centrifuged at 4000 rpm for 10 min, Chl-*a*  
129 was measured using a standard fluorometric method with a Turner Designs fluorometer (Parsons et al.,  
130 1984). Water samples for nutrients were filtered through 0.45  $\mu\text{m}$  Nucleopore filters and stored at -20 °C.  
131 Nutrient concentrations including nitrate plus nitrite, phosphate, and silicate were measured using a  
132 segmented-flow nutrient autoanalyzer (Seal AA3, Bran-Luebbe, GmbH).

133

### 134 **2.3 Sampling and measurements of particulate and dissolved PUAs in one-liter seawater**

135 We used a similar protocol of Wu and Li (2016) for pPUAs and dPUAs collection, pretreatment, and  
136 determination. Briefly, 2-4 liters of water sample went through a GF/C filtration with both the filter and the  
137 filtrate collected separately. The filter was rinsed by the derivative solution with the suspended particle  
138 samples collected in a glass vial. After adding internal standard, the samples in the vial were frozen and  
139 thawed three times to mechanically break the cells for pPUAs. The filtrate from the GF/C filtration was  
140 also added with internal standard and transferred to a C18 solid-phase extraction cartridge. The elute from  
141 the cartridge with the derivative solution was saved in a glass vial for dPUAs. Both pPUAs and dPUAs  
142 samples were frozen and stored at -20 °C.

143 In the laboratory, the pPUAs sample was thawed with the organic phase extracted. After the solvent  
144 was evaporated with the sample concentrated and re-dissolved in hexane, pPUAs was determined using gas  
145 chromatography and mass spectrometry (Agilent Technologies Inc., USA). Standards series were prepared  
146 by adding certain amounts of three major PUAs to the derivative solution and went through the same  
147 pretreatment and extraction steps as samples. Derivatives of dPUAs were extracted and measured by  
148 similar methods as pPUAs, except that the calibration curves of dPUAs were constructed separately. The  
149 units of pPUAs and dPUAs are  $\text{nmol L}^{-1}$  (nmol PUA in one-liter seawater).

150

### 151 **2.4 Particle collections by large-volume filtrations in hypoxia waters.**

152 Large volumes (~300 L) of the middle (12 m) and the bottom (25 m) waters within the hypoxia zone were  
153 collected by Niskin bottles at station Y1. For each layer, the water sample was quickly filtered through a  
154 sterile fabric screen (25  $\mu\text{m}$  filter) on a disk filter equipped with a peristaltic pump to qualitatively obtain  
155 particles of >25  $\mu\text{m}$ . Larger zooplankters were picked off immediately. The particle samples were gently  
156 back-flushed three times off the fabric screen using particle-free seawater (obtained using a 0.2  $\mu\text{m}$   
157 filtration of the same local seawater) into a sterile 50-mL sampling tube.

158 The volume of total particles from large-volume-filtration was measured as follows: The collected  
159 particle in the 50 mL tube was centrifuged for one minute at a speed of 3000 revolutions per minute (r.p.m)  
160 with the supernatant saved (Hmelo et al., 2011). The particle sample was resuspended as slurry by gently  
161 shaking and transferred into a sterile 5 mL graduated centrifuge tube. The sample was centrifuged again by  
162 the same centrifuging speed with the final volume of the total particles recorded. The unit for the total  
163 particle volume is mL.

164 All the particles were transferred back to the sterile 50 mL centrifuge tube (so as all the supernatants)  
165 with 0.2- $\mu$ m-filtered seawater, which was used for subsequent measurements of particle-adsorbed PUAs as  
166 well as for PUAs-amended incubation experiments of particle-attached bacteria.

167

## 168 **2.5 Measurements of particle-adsorbed PUAs**

169 After gently shaking, 3 mL of sample in the 50 mL sampling tube (see section 2.4) was used for the  
170 analyses of particle-adsorbed PUAs concentration (two replicates) according to the procedure shown in  
171 Figure 2 (modified from the protocols of Edwards et al. 2015 and Wu and Li 2016). The sample (3 mL) was  
172 transferred to 50 mL centrifuge tubes for PUAs derivatization on board. An internal standard of  
173 benzaldehyde was added to obtain a final concentration of 10  $\mu$ M. The aldehydes in the samples were  
174 derivatized by the addition of O-(2,3,4,5,6-pentafluorobenzyl) hydroxylamine hydrochloride solution in  
175 deionized water ( $pH=7.5$ ). The reaction was performed at room temperature for 15 min (shaking slightly  
176 for mix every 5 min). Then 2 mL sulfuric acid (0.1%) solution was added to a final concentration of 0.01%  
177 acid ( $pH$  of 2-3) to avoid new PUAs induced by enzymatic cascade reactions. The derivate samples were  
178 subsequently sonicated for 3 min before the addition of 20 mL hexane, and the upper organic phase of the  
179 extraction was transferred to a clean tube and stored at  $-20$  °C.

180 Upon returning to the laboratory, the adsorbed PUAs on these particles (undisrupted PUAs) were  
181 determined with the same analytical methods as those for the disrupted pPUAs (freeze-thaw methods to  
182 include the portion of PUAs eventually produced as cells die, Wu and Li 2016) except for the freeze-thaw



183 step. A separate calibration curve was made for the undisrupted PUAs derivatives. A standard series of  
184 heptadienal, octadienal, and decadienal (0, 0.1, 0.5, 1.0, 2.5, 5.0, 10.0, 25.0 nmol L<sup>-1</sup>) was prepared before  
185 each analysis by diluting a relevant amount of the PUA stock solution (methanolic solution) with deionized  
186 water. These standard solutions were processed through all the same experimental steps as those mentioned  
187 above for derivation, extraction, and measurement of the undisrupted PUAs sample. The unit for the  
188 undisrupted PUAs is nmol L<sup>-1</sup>. The total amount of the undisrupted PUAs in the 50 mL sampling tube was  
189 the product of the measured concentration and the total volume of the sample.

190 The hotspot PUAs concentration associated with the aggregate particles is defined as the PUAs  
191 concentration in the volume of the water parcel displaced by these particles. Therefore, the final  
192 concentration of particle-adsorbed PUAs in the water column, defined as PUAs [ $\mu\text{mol L}^{-1}$ ], should be equal  
193 to the moles of particle-adsorbed PUAs (nmol, the undisrupted PUAs) divided by the volume of particles  
194 (mL).

195

## 196 **2.6 Incubation of particle-attached bacteria with PUAs treatments.**

197 The impact of PUAs on microbial growth and metabolisms in the hypoxia zone was assessed by field  
198 incubation of particle-attached bacteria on particles of > 25  $\mu\text{m}$  collected from large-volume filtration with  
199 direct additions of low or high doses of PUAs (1 or 100  $\mu\text{mol L}^{-1}$ ) on June, 29<sup>th</sup>, 2019 (Figure 2).

200 A sample volume of ~32 mL in the centrifuge tube (section 2.4) was transferred to a sterile Nalgene  
201 bottle before being diluted by particle-free seawater to a final volume of 4 L. About 3.2 L of the sample  
202 solution was transferred into four sterile 1-L Nalgene bottles (each with 800 mL). One 1-L bottle was used  
203 for determining the initial conditions: after gentle shaking, the solution was transferred into six biological  
204 oxygen demand (BOD) bottles with three for initial oxygen concentration (fixed immediately by Winkler  
205 reagents) and the other three for initial bacterial abundance, production, and community structure. The  
206 other three 1-L bottles were used for three different treatments (each with two replicates in two 0.5-L  
207 bottles): the first one served as the control with the addition of 200  $\mu\text{L}$  methanol, the second one with 200

208  $\mu\text{L}$  low-dose PUAs solution, and the third one with 200  $\mu\text{L}$  high-dose PUAs solution (Table 1). We should  
209 note that the methanol percentage (0.05% v/v) here is higher than its natural level in seawater although no  
210 substantial change of bacterial community was found.

211 \_The solution in each of the three treatments (0.5L bottles) was transferred to six parallel replicates by  
212 60-mL BOD bottles. These BOD bottles were incubated at *in situ* temperature in the dark for 12 hours. At  
213 the end of each incubation experiment, three of the six BOD bottles were used for determining the final  
214 oxygen concentrations with the other three for the final bacterial abundance, production, and community  
215 structure.

216 To test the possibility of PUAs as carbon sources for bacterial utilization, a minimal medium was  
217 prepared with only sterile artificial seawater but not any organic carbons (Dyksterhouse et al., 1995). A  
218 volume of 375  $\mu\text{L}$  sample (from the above 4 L sample solution) was inoculated in the minimal medium  
219 amended with heptadienal in a final concentration of about 200  $\mu\text{mol L}^{-1}$ . This PUA level was close to the  
220 hotspot PUAs of 240  $\mu\text{mol L}^{-1}$  found in the suspended particles of a station near the PRE. It was also  
221 comparable to the hotspot PUAs of 25.7  $\mu\text{mol L}^{-1}$  in the temperate west North Atlantic (Edwards et al.,  
222 2015). For comparisons, the same amount of sample was also inoculated in the minimal medium (75 mL)  
223 amended with an alkane mixture (ALK, n-pentadecane and n-heptadecane) at a final concentration of 0.25  
224  $\text{g L}^{-1}$ , or with a mixture of polycyclic aromatic hydrocarbons (PAH, naphthalene and phenanthrene) at a  
225 final concentration of 200 ppm. These experiments were performed in dark at room temperature for over 30  
226 days. Significant turbidity changes in the cell culture bottle over incubation time will be observed if there is  
227 a carbon source for bacterial growth.

## 229 **2.7 Measurements of bacteria-related parameters**

### 230 **(1) Bacterial abundance**

231 At the end of the 12-h incubation period, a 2 mL sample from each BOD bottle was preserved in 0.5%  
232 glutaraldehyde. The fixation lasted for half of an hour at room temperature before being frozen in liquid  $\text{N}_2$

233 and stored in a  $-80^{\circ}\text{C}$  freezer. In the laboratory, the samples were performed through a previously  
234 published procedure for detaching particle-attached bacteria (Lunau et al., 2005), which had been proved  
235 effective for samples with high particle concentrations. To break up particles and attached bacteria, 0.2 mL  
236 pure methanol was added to the 2 mL sample and vortexed. The sample was then incubated in an ultrasonic  
237 bath (35 kHz, 2 x 320W per period) at  $35^{\circ}\text{C}$  for 15 min. Subsequently, the tube sample was filtered with a  
238  $50\ \mu\text{m}$ -filter to remove large detrital particles. The filtrate samples for surface-associated bacteria cells  
239 were diluted by 5-10 folds using TE buffer solution and stained with 0.01% SYBR Green I in the dark at  
240 room temperature for 40 min. With the addition of  $1\text{-}\mu\text{m}$  beads, bacterial abundance (BA) of the samples  
241 was counted by a flow cytometer (Beckman Coulter CytoFlex S) with bacteria detected on a plot of green  
242 fluorescence versus side scatter (Marie et al., 1997). The precision of the method estimated by the  
243 coefficient of variation (CV%) was generally less than 5%.

244 For bulk-water bacteria abundance, 1.8 mL of seawater sample was collected after a  $20\text{-}\mu\text{m}$   
245 prefiltration. The sample was transferred to a 2 mL centrifuge tube and fixed by adding  $20\ \mu\text{L}$  of 20%  
246 paraformaldehyde before storage in a  $-80^{\circ}\text{C}$  freezer. In the laboratory,  $300\ \mu\text{L}$  of the sample after thawing  
247 was used for staining with SYBR Green and analyzed using the same flow cytometry method as above  
248 (Marie, et al, 1997).

249

## 250 **(2) Bacterial respiration**

251 For BOD samples, bacterial respiration (BR) was calculated based on the oxygen decline during the 12-h  
252 incubation and was converted to carbon units with the respiratory quotient assumed equal to 1 (Hopkinson,  
253 1985). Dissolved oxygen was determined by a high-precision Winkler titration apparatus (Metrohm-848,  
254 Switzerland) based on the classic method (Oudot et al., 1988). We should mention that BR could be  
255 overestimated if phytoplankton and microzooplankton were present in the particle aggregates of  $> 25\ \mu\text{m}$ .  
256 However, this effect could be relatively small because the raw seawater in the hypoxic zone had very low

257 chlorophyll-*a* and because there was virtually not much microzooplankton in the sample (confirmed by  
258 FlowCAM).

259 Method for the estimation of the bulk water bacterial respiration at stations X1, X2, and X3 can be  
260 found in Xu et al (2018). For the bulk water at station Y1, the size-fractionated respiration rates, including  
261 free-living bacteria of 0.2-0.8  $\mu\text{m}$  and particle-associated community of  $>0.8 \mu\text{m}$  (we assumed that they  
262 were mostly PAB given the low phytoplankton chlorophyll-*a* of the sample and the absence of zooplankton  
263 during the filtration), were estimated based on the method of García-Martín et al (2019). Four 100 mL  
264 polypropylene bottles were filled with seawater. One bottle was immediately fixed by formaldehyde. After  
265 15 min, the sample in each bottle was incubated in the dark at the *in situ* temperature after the addition of  
266 the Iodo-Nitro-Tetrazolium (INT) salt at a final concentration of  $0.8 \text{ mmol L}^{-1}$ . The incubation reaction  
267 lasted for 1.5 h before being stopped by formaldehyde. After 15 min, all the samples were sequentially  
268 filtered through 0.8 and 0.2  $\mu\text{m}$  pore size polycarbonate filters and stored frozen until further measurements  
269 by spectrophotometry.

270

### 271 **(3) Bacterial production**

272 Bacterial production (BP) was determined using a modified protocol of the  $^3\text{H}$ -leucine incorporation  
273 method (Kirchman, 1993). Four 1.8-mL aliquots of the sample were collected by pipet from each BOD  
274 incubation and added to 2-mL sterile microcentrifuge tubes, which were incubated with  $^3\text{H}$ -leucine (in a  
275 final concentration of  $4.65 \mu\text{mol Leu L}^{-1}$ , Perkin Elmer, USA). One tube served as the control was fixed by  
276 adding 100% trichloroacetic acid (TCA) immediately (in a final concentration of 5%). The other three were  
277 terminated with TCA at the end of the 2-h dark incubation. Samples were filtered onto 0.2- $\mu\text{m}$   
278 polycarbonate filters and then rinsed twice with 5% TCA and three times with 80% ethanol (Huang et al.,  
279 2018) before being stored at  $-80 \text{ }^\circ\text{C}$ . In the laboratory, the filters were transferred to scintillation vials with  
280 5 mL of Ultima Gold scintillation cocktail. The incorporated  $^3\text{H}$  was determined using a Tri-Carb 2800TR  
281 liquid scintillation counter. Bacterial production was calculated with the previous published

282 leucine-to-carbon empirical conversion factors of  $0.37 \text{ kg C mol leucine}^{-1}$  in the study area (Wang et al.,  
283 2014). Bacterial carbon demand (BCD) was calculated as the sum of BP and BR. Bacterial growth  
284 efficiency (BGE) was equated to BP/BCD.

285

#### 286 **(4) Bacterial community structure**

287 At the end of incubation, the DNA sample was obtained by filtering 30 mL of each BOD water via a  
288 0.22- $\mu\text{m}$  Millipore filter, which was preserved in a cryovial with the DNA protector buffer and stored at  
289  $-80 \text{ }^\circ\text{C}$ . DNA was extracted using the DNeasy PowerWater Kit with genomic amplification by Polymerase  
290 Chain Reaction (PCR). The V3 and V4 fragments of bacterial 16S rRNA were amplified at  $94 \text{ }^\circ\text{C}$  for 2 min  
291 and followed by 27 cycles of amplification ( $94 \text{ }^\circ\text{C}$  for 30 s,  $55^\circ \text{C}$  for 30 s, and  $72 \text{ }^\circ\text{C}$  for 60 s) before a  
292 final step of  $72 \text{ }^\circ\text{C}$  for 10 min. Primers for amplification included 341F (CCTACGGGNGGCWGCAG) and  
293 805R (GACTACHVGGGTATCTAATCC). Reactions were performed in a 10- $\mu\text{L}$  mixture containing 1  $\mu\text{L}$   
294 Toptaq Buffer, 0.8  $\mu\text{L}$  dNTPs, 10  $\mu\text{M}$  primers, 0.2  $\mu\text{L}$  Taq DNA polymerase, and 1  $\mu\text{L}$  Template DNA.  
295 Three parallel amplification products for each sample were purified by an equal volume of AMPure XP  
296 magnetic beads. Sample libraries were pooled in equimolar and paired-end sequenced ( $2 \times 250 \text{ bp}$ ) on an  
297 Illumina MiSeq platform.

298 High-quality sequencing data was obtained by filtering on the original off-line data. Briefly, the raw  
299 data was pre-processed using TrimGalore to remove reads with qualities of less than 20 and FLASH2 to  
300 merge paired-end reads. Besides, the data were also processed using Usearch to remove reads with a total  
301 base error rate of greater than 2 and short reads with a length of less than 100 bp and using Mothur to  
302 remove reads containing more than 6 bp of N bases. We further used UPARSE to remove the singleton  
303 sequence to reduce the redundant calculation during the data processing. Sequences with similarity greater  
304 than 97% were clustered into the same operational taxonomic units (OTUs). R software was used for  
305 community composition analysis.

306 DNA samples for the bulk bacteria ( $>0.2 \text{ }\mu\text{m}$ ) and PAB on particles of  $> 25 \text{ }\mu\text{m}$  at station Y1 were also

307 collected for bacterial community analysis using the same method described above. Methods for the bulk  
308 water bacterial community analyses at stations X1, X2, and X3 during the 2016 cruise can be found in the  
309 published paper of Xu et al. (2018).

310

## 311 **2.8 Statistical Analysis**

312 All statistical analyses were performed using the statistical software SPSS (Version 13.0, SPSS Inc.,  
313 Chicago, IL, USA). A student's t-test with a 2-tailed hypothesis was used when comparing PUAs-amended  
314 treatments with the control or comparing stations inside and outside the hypoxic zone, with the null  
315 hypothesis being rejected if the probability ( $p$ ) is less than 0.05. We consider  $p$  of  $<0.05$  as significant and  $p$   
316 of  $<0.01$  as strong significant. Ocean Data View with the extrapolation model "DIVA Gridding" method  
317 was used to contour the spatial distributions of physical and biogeochemical parameters.

318

## 319 **3. Results**

### 320 **3.1 Characteristics of hydrography, biogeochemistry, and bulk bacteria community in the hypoxic** 321 **zone**

322 During our study periods, there was a large body of low oxygen bottom water with the strongest hypoxia ( $<$   
323  $62.5 \mu\text{mol kg}^{-1}$ ) on the western shelf of the PRE (Figure 1), which was relatively similar among different  
324 summers of 2016 and 2019 (Figure 1). For vertical distribution, a strong salt-wedge structure was found  
325 over the inner shelf (Figures 3A, 3D) with freshwater on the shore side due to intense river discharge.  
326 Bottom waters with oxygen deficiency ( $< 93.5 \mu\text{mol kg}^{-1}$ ) occurred below the lower boundary of the  
327 salt-wedge and expanded  $\sim 60$  km offshore (Figure 3E). In contrast, a surface high Chl- $a$  patch ( $6.3 \mu\text{g L}^{-1}$ )  
328 showed up near the upper boundary of the front, where there was enhanced water-column stability, low  
329 turbidity, and high nutrients (Figures 3B, 3C). Therefore, there was a spatial mismatch between the  
330 subsurface hypoxic zone (Figure 3E) and the surface chlorophyll-bloom (Figure 3F) during the  
331 estuary-to-shelf transect, as both the surface Chl- $a$  and oxygen right above the hypoxic zones at the bottom

332 boundary of the salt-wedge were not themselves maxima.

333 There were much higher rates of respiration (BR) ( $t=7.8$ ,  $n=9$ ,  $p<0.01$ ) and production (BP) ( $t=13.0$ ,  
334  $n=9$ ,  $p<0.01$ ) for the bulk bacterial community (including FLB and PAB) in the bottom waters of X1 within  
335 the hypoxic core than those of X2 and X3 outside the hypoxic zone during June 2016 (Figure 4, modified  
336 from data of Xu et al., 2018). The size-fractionated respiration rates were quantified at station Y1 during the  
337 2019 cruise (Figure S1) to distinguish the different roles of FLB and PAB on bacterial respiration in the  
338 hypoxic waters. Our results suggested that bacterial respiration within the hypoxic waters was largely  
339 contributed by PAB ( $>0.8 \mu\text{m}$ ), which was about 2.3-3 folds of that by FLB (0.2-0.8  $\mu\text{m}$ ).

340 The bulk bacterial composition of the bottom water of X1 during the 2016 cruise with 78% of  
341  $\alpha$ -Proteobacteria ( $\alpha$ -Pro), 15% of  $\gamma$ -Proteobacteria ( $\gamma$ -Pro), and 6% of Bacteroidetes was significantly  
342 different from those of X2 and X3 (91%  $\alpha$ -Pro, 5%  $\gamma$ -Pro, and 2% Bacteroidetes), although their bacterial  
343 abundances were about the same (Figure 4). Compared to that of the 2016 cruise, there was a different  
344 taxonomic composition of the bulk bacterial community in the hypoxic waters of the 2019 cruise with on  
345 average 33% of  $\alpha$ -Pro, 25% of  $\gamma$ -Pro, and 14% of Bacteroidetes. Furthermore, there was a substantially  
346 different taxonomic composition for PAB ( $>25 \mu\text{m}$ ) with on average 66% of  $\gamma$ -Pro, 22% of  $\alpha$ -Pro, and 4%  
347 of Bacteroidetes (Figure S2A). In particular, there was an increase of  $\gamma$ -Pro, but a decrease of  $\alpha$ -Pro and  
348 Bacteroidetes, in the PAB ( $>25 \mu\text{m}$ ) relative to the bulk bacterial community. On the genus level, the PAB  
349 ( $>25 \mu\text{m}$ ) was largely dominated by the *Alteromonas* group in both the middle and bottom waters (Figure  
350 S2B).

351

### 352 **3.2 PUAs concentrations in the hypoxic zone**

353 Generally, there were significantly higher pPUAs of  $0.18 \text{ nmol L}^{-1}$  ( $t=3.20$ ,  $n=10$ ,  $p<0.01$ ) and dPUAs of  
354  $0.12 \text{ nmol L}^{-1}$  ( $t=7.61$ ,  $n=8$ ,  $p<0.01$ ) in the hypoxic waters than in the nearby bottom waters without  
355 hypoxia ( $0.02 \text{ nmol L}^{-1}$  and  $0.01 \text{ nmol L}^{-1}$ ). Vertical distributions of pPUAs and dPUAs in the bulk seawater  
356 were showed for two stations (Y1 and Y2) inside and outside the hypoxic zone (Figure 1). Nanomolar

357 levels of pPUAs and dPUAs were found in the water column in both stations (Figures 5E, 5F). There were  
358 high pPUAs and dPUAs in the bottom hypoxic waters of station Y1 (Figure 5E, 5F) together with locally  
359 elevated turbidity (Figure 3B) when compared to the bottom waters outside, which likely a result of particle  
360 resuspension. For station Y2 outside the hypoxia, we found negligible pPUAs and dPUAs at depths below  
361 the mixed layer (Figure 5E, 5F), which could be due to PUAs dilution by the intruded subsurface seawater.

362 Particle-adsorbed PUAs in the low-oxygen waters were quantified for the first time with the direct  
363 particle volume estimated by large-volume-filtration (see the method section), which would reduce the  
364 uncertainty associated with particle volume calculated by empirical equations derived for marine-snow  
365 particles (Edward et al., 2015). We found high levels of particle-adsorbed PUAs ( $\sim 10 \mu\text{mol L}^{-1}$ ) in these  
366 waters (Figure 6), which were orders of magnitude higher than the bulk water pPUAs or dPUAs  
367 concentrations ( $< 0.3 \text{ nmol L}^{-1}$ , Figure 5E, 5F). Particle-adsorbed PUAs of the low-oxygen waters mainly  
368 consisted of heptadienal (C7\_PUA) and octadienal (C8\_PUA).

369

### 370 **3.3 Particle-attached bacterial growth and metabolism in the hypoxic zone**

371 Incubation of the PAB acquired from the low-oxygen waters with direct additions of different doses of  
372 exogenous PUAs over 12 hours was carried out to examine the change of bacterial growth and metabolism  
373 activities in response to PUA-enrichments. At the end of the incubation experiments, BA was not different  
374 from the control for the PH treatment (Figure 7A). However, for the PL treatment, there were substantial  
375 increases of BA in both the middle and the bottom waters compared to the initial conditions (Figure 7A). In  
376 particular, BA of  $\sim 3.2 \pm 0.04 \times 10^9 \text{ cells L}^{-1}$  in the bottom water for the PL treatment was significantly  
377 higher ( $t=12.26$ ,  $n=12$ ,  $p<0.01$ ) than the control of  $2.5 \pm 0.07 \times 10^9 \text{ cells L}^{-1}$ .

378 BR was significantly promoted by the low-dose PUAs with a 21.6% increase in the middle layer  
379 ( $t=11.91$ ,  $n=8$ ,  $p<0.01$ ) and a 25.8% increase in the bottom layer ( $t=11.50$ ,  $n=8$ ,  $p<0.01$ ) compared to the  
380 controls. Stimulating effect of high-dose PUAs on BR was even stronger with 47.0% increase in the middle  
381 layer ( $t=30.56$ ,  $n=8$ ,  $p<0.01$ ) and 39.8% increase in the bottom layer ( $t=9.40$ ,  $n=8$ ,  $p<0.01$ ) (Figure 7B).



382 Meanwhile, the cell-specific BR was significantly improved for both layers with high-dose of PUAs  
383 ( $t=15.13$ ,  $n=8$ ,  $p<0.01$  and  $t=4.77$ ,  $n=8$ ,  $p<0.01$ ), but not with low-dose of PUAs (Figure 7C) due to  
384 increase of BA (Figure 7A). BGE was generally very low (<1.5%) during all the experiments (Figure 7D)  
385 due to substantially high rates of BR (Figure 7B) than BP (Figure 7E). Also, there was no significant  
386 difference in BGE between controls and PUAs treatments for both layers (Figure 7D).

387 For the bottom layer, BP was  $12.6 \pm 0.8 \mu\text{g C L}^{-1} \text{d}^{-1}$  for low-dose PUAs and  $16.4 \pm 0.6 \mu\text{g C L}^{-1} \text{d}^{-1}$   
388 for high-dose PUAs, which were both significantly ( $t=2.98$ ,  $n=8$ ,  $p<0.05$  and  $t=10.41$ ,  $n=8$ ,  $p<0.01$ ) higher  
389 than the control of  $10.6 \pm 0.6 \mu\text{g C L}^{-1} \text{d}^{-1}$ . Meanwhile, BP in the middle layer was significantly higher  
390 ( $t=2.52$ ,  $n=8$ ,  $p<0.05$ ) than the control for high-dose PUAs ( $13.4 \pm 0.9 \mu\text{g C L}^{-1} \text{d}^{-1}$ ) but not for low-dose  
391 PUAs ( $12.6 \pm 0.9 \mu\text{g C L}^{-1} \text{d}^{-1}$ ) (Figure 7E). The cell-specific BP (sBP,  $7.9 \pm 0.5$  and  $6.9 \pm 0.2 \text{ fg C cell}^{-1} \text{d}^{-1}$ )  
392 for high-dose PUAs were significantly ( $t=2.62$ ,  $n=8$ ,  $p<0.05$  and  $t=11.26$ ,  $n=8$ ,  $p<0.01$ ) higher than the  
393 control in both layers (Figure 7F). Meanwhile, for low-dose PUAs, the sBP in both layers were not  
394 significantly different from the controls.

395

### 396 **3.4 Particle-attached bacterial community change during incubations**

397 Generally,  $\gamma$ -Pro dominated (>68%) the bacterial community at the class level for all experiments, followed  
398 by the second largest bacterial group of  $\alpha$ -Pro. There was a significant increase of  $\gamma$ -Pro by high-dose PUAs  
399 with increments of 17.2% ( $t=9.25$ ,  $n=8$ ,  $p<0.01$ ) and 19.5% ( $t=6.32$ ,  $n=8$ ,  $p<0.01$ ) for the middle and the  
400 bottom layers, respectively (Figure 8A). However, there was no substantial change of bacterial community  
401 composition by low-dose PUAs for both layers (Figure 8A).

402 On the genus level, there was also a large difference in the responses of various bacterial subgroups to  
403 the exposure of PUAs (Figure 8B). The main contributing genus for the promotion effect by high-dose  
404 PUAs was the group of *Alteromonas* spp., which showed a large increase in abundance by 73.9% and  
405 69.7% in the middle and the bottom layers. For low-dose PUAs, the promotion effect of PUAs on  
406 *Alteromonas* spp. was still found although with a much lower intensity (5.4% in the middle and 19.4% in

407 the bottom). The promotion effect of  $\gamma$ -Pro by high-dose PUAs was also contributed by bacteria *Halomonas*  
408 spp. (percentage increase from 1.7% to 7.4%). Meanwhile, some bacterial genus, such as *Marinobacter* and  
409 *Methylophaga* from  $\gamma$ -Pro, or *Nautella* and *Sulfitobacter* from  $\alpha$ -Pro, showed decreased percentages by  
410 high-dose PUAs (Figure 8B).

411

### 412 **3. 5 Carbon source preclusion experiments for PUAs**

413 After one month of incubation, PAB inoculated from the low-oxygen waters showed dramatic responses to  
414 both PAH and ALK (Figure 9). In particular, the mediums of PAH addition became turbid brown (bottles on  
415 the left) with the medium of ALK addition turning into milky white (bottles in the middle) (Figures 9B and  
416 9D). For comparison, they were both clear and transparent at the beginning of the experiments (Figures 9A  
417 and 9C). These results should reflect the growth of bacteria in these bottles with the enrichments of organic  
418 carbons. Meanwhile, the minimal medium with the addition of heptadienal (C7\_PUA) remained clear and  
419 transparent as it was originally, which would indicate that PAB did not grow in the treatment of C7\_PUA.

420

## 421 **4. Discussion**

422 Hypoxia occurs if the rate of oxygen consumption exceeds that of oxygen replenishment by diffusion,  
423 mixing, and advection (Rabouille et al., 2008). The spatial mismatch between the surface chlorophyll-*a*  
424 maxima and the subsurface hypoxia during our estuary-to-shelf transect should indicate that the  
425 low-oxygen feature may not be directly connected to particle export by the surface phytoplankton bloom.  
426 This outcome can be a combined result of riverine nutrient input in the surface, water-column stability  
427 driven by wind and buoyancy forcing, and flow convergence for an accumulation of organic matters in the  
428 bottom (Lu et al., 2018).

429 Elevated concentrations of pPUAs and dPUAs near the bottom boundary of the salt-wedge should  
430 reflect a sediment source of PUAs, as the surface phytoplankton above them was very low. PUA-precursors  
431 such as PUFA could be accumulated as detritus in the surface sediment near the PRE mouth during the

432 spring blooms (Hu et al., 2006). Strong convergence at the bottom of the salt-wedge could be driven by  
433 shear vorticity and topography (Lu et al., 2018). This would allow for the resuspension of small detrital  
434 particles. Improved PUAs production by oxidation of the resuspended PUFA could occur below the  
435 salt-wedge as a result of enhanced lipoxygenase activity (in the resuspended organic detritus) in response to  
436 salinity increase by the intruded bottom seawater (Galeron et al., 2018).

437 Direct measurement of the adsorbed PUAs concentration associated with the suspended particles  
438 of  $>25\ \mu\text{m}$  by the method of combined large-volume filtration and on-site derivation and extraction yield a  
439 high level of  $\sim 10\ \mu\text{mol L}^{-1}$  within the hypoxic zone. This value is comparable to those previously reported  
440 in sinking particles ( $>50\ \mu\text{m}$ ) of the open ocean using particle-volume calculated from diatom-derived  
441 marine snow particles (Edward et al., 2015). Note that there was also a higher level of  $240\ \mu\text{mol L}^{-1}$  found  
442 in another station outside the PRE. A micromolar level of particle-adsorbed PUAs could act as a hotspot for  
443 bacteria likely exerting important impacts as signaling molecules on microbial utilization of particulate  
444 organic matters and subsequent oxygen consumption.

445 It should be mentioned that various pore sizes have been used for PAB sampling in the literature. A  
446  $0.8\text{-}\mu\text{m}$  filtration was generally accepted for separating PAB ( $>0.8\ \mu\text{m}$ ) and FLB ( $0.2\text{-}0.8\ \mu\text{m}$ ) in the ocean  
447 (Robinson and Williams, 2005; Kirchman, 2008; Huang et al., 2018; Liu et al., 2020). Other studies defined  
448 size of  $>3\ \mu\text{m}$  for PAB and  $0.2\text{-}3\ \mu\text{m}$  for FLB in some coastal waters (Crump et al. 1999; Garneau et al.,  
449 2009; Zhang et al., 2016). Meanwhile, there were also many studies using much larger sizes of filtration for  
450 PAB: a  $5\text{-}\mu\text{m}$  filter in the German Wadden Sea (Rink et al. 2003), a  $10\text{-}\mu\text{m}$  filter in the Santa Barbara  
451 Channel (DeLong et al. 1993), a  $30\text{-}\mu\text{m}$  filter in the Black Sea (Fuchsman et al., 2011), and a  $50\text{-}\mu\text{m}$ -mesh  
452 nylon net in the North Atlantic waters (Edwards et al., 2015).

453 The hypoxic waters below the salt-wedge have high turbidity probably due to particle resuspension.  
454 High particle concentration here may explain the pervious finding of a higher abundance of PAB than FLB  
455 in the same area (e.g. Li et al., 2018; Liu et al., 2020), similar to those found in the Columbia River estuary  
456 (Crump et al., 1998). Also, anaerobic bacteria and taxa preferring low-oxygen conditions were found more

457 enriched in the particle-attached communities than their free-living counterparts in the PRE (Zhang et al.,  
458 2016). Our field measurements suggested that bacterial respiration within the hypoxic waters was largely  
459 contributed by PAB ( $>0.8 \mu\text{m}$ ) with FLB ( $0.2\text{-}0.8 \mu\text{m}$ ) playing a relatively small role. Therefore, it is  
460 crucial to address the linkage between the high-density PAB and the high level of particle-adsorbed PUAs  
461 associated with the suspended particles in the low-oxygen waters.

462 We choose a larger pore-size of  $25 \mu\text{m}$  for collecting bacteria attached to sinking aggregates and large  
463 suspended particles. Firstly, it has been suggested that microbial respiration rate can be positively related to  
464 aggregate size (Ploug et al., 2002) and thus larger PAB likely contributes more to oxygen consumption.  
465 Secondly, larger particle size can better present the PAB taxonomy according to the previous finding of the  
466 saturation of species-accumulation (for the size-fractionated bacteria) when the size is greater than  $20 \mu\text{m}$   
467 (Mestre et al., 2017). Thus, the taxonomic groups of PAB caught on particles of  $>25 \mu\text{m}$  should already  
468 cover those of PAB on smaller particles of  $0.8\text{-}25 \mu\text{m}$ . A similar type of filtration ( $30 \mu\text{m}$ ) has been  
469 previously applied to study PAB in the Black Sea suboxic zones (Fuchsman et al., 2011).

470 Interestingly, our PUA-amended experiments for PAB ( $>25 \mu\text{m}$ ) retrieved from the low-oxygen waters  
471 revealed distinct responses of PAB to different doses of PUAs treatments with an increase in cell growth in  
472 response to low-dose PUAs ( $1 \mu\text{mol L}^{-1}$ ) but an elevated cell-specific metabolic activity including bacterial  
473 respiration and production in response to high-dose PUAs ( $100 \mu\text{mol L}^{-1}$ ). An increase in cell density of  
474 PAB by low-dose PUAs could likely reflect the stimulating effect of PUAs on PAB growth. This finding  
475 was consistent with the previous report of a PUAs level of  $0\text{-}10 \mu\text{mol L}^{-1}$  stimulating respiration and cell  
476 growth of PAB in sinking particles of the open ocean (Edwards et al., 2015). The negligible effect of  
477 low-dose PUAs on bacterial community structure in our experiments was also in good agreement with  
478 those found for PAB from sinking particles (Edwards et al., 2015). However, we do not see the inhibitory  
479 effect of  $100 \mu\text{mol L}^{-1}$  PUAs on PAB respiration and production previously found in the open ocean  
480 (Edward et al., 2015). Instead, the stimulating effect for high-dose PUAs on bacterial respiration and  
481 production was even stronger with  $\sim 50\%$  increments. The bioactivity of PUAs on bacterial strains could

482 likely arise from its specific arrangement of two double bonds and carbonyl chain (Ribalet et al., 2008).  
483 Our findings support the important role of PUAs in enhancing bacterial oxygen utilization in low-oxygen  
484 waters.

485 It should be mentioned that it remains controversial the effect of background nanomolar PUAs on  
486 free-living bacteria, which is not our focus in this study. Previous studies suggested that 7.5 nmol L<sup>-1</sup> PUAs  
487 would have a different effect on the metabolic activities of distinct bacterial groups in the NW  
488 Mediterranean Sea, although bulk bacterial abundance remained unchanged (Balestra et al., 2011). In  
489 particular, the metabolic activity of  $\gamma$ -Pro was least affected by nanomolar PUAs, although those of  
490 Bacteroidetes and Rhodobacteraceae were markedly depressed (Balestra et al., 2011). Meanwhile, the daily  
491 addition of 1 nmol L<sup>-1</sup> PUAs was found to not affect the bacterial abundance and community composition  
492 during a mesocosm experiment in the Bothnian Sea (Paul et al., 2012).

493 It is important to verify that the PUAs are not an organic carbon source but a stimulator for PAB  
494 growth and metabolism. This was supported by the fact that the inoculated PAB could not grow in the  
495 medium with 200  $\mu$ mol L<sup>-1</sup> of PUAs although they grew pretty well in the mediums with a similar amount  
496 of ALK or PAH. Our results support the previous findings that the density of *Alteromonas hispanica* was  
497 not significantly affected by 100  $\mu$ mol L<sup>-1</sup> of PUAs in the minimal medium (without any organic carbons)  
498 during laboratory experiments (Figure 9E), where PUAs were considered to act as cofactors for bacterial  
499 growth (Ribalet et al., 2008).

500 Improved cell-specific metabolism of PAB in response to high-dose PUAs was accompanied by a  
501 significant shift of bacterial community structure. The group of PAB with the greatest positive responses to  
502 exogenous PUAs was genus *Alteromonas* within the  $\gamma$ -Pro, which is well-known to have a particle-attached  
503 lifestyle with rapid growth response to organic matters (Ivars-Martinez et al., 2008). This result is  
504 contradicted by the previous finding of a reduced percentage of the  $\gamma$ -Pro class by high-dose PUAs in the  
505 PAB of open ocean sinking particles (Edward et al., 2015). Meanwhile, previous studies suggested that  
506 different genus groups within the  $\gamma$ -Pro may respond distinctly to PUAs (Ribalet et al., 2008). Our result

507 was well consistent with the previous finding of the significant promotion effect of 13 or 106  $\mu\text{mol L}^{-1}$   
508 PUAs on *Alteromonas hispanica* from the pure culture experiment (Ribalet et al., 2008). An increase of  
509 PUAs could thus confer some of the  $\gamma$ -Pro (mainly special species within the genus *Alteromonas*, such as *A.*  
510 *hispanica*, Figure S2B) a competitive advantage over other bacteria, leading to their population dominance  
511 on particles in the low-oxygen waters. These results provide evidences for a previous hypothesis that PUAs  
512 could shape the bacterioplankton community composition by driving the metabolic activity of bacteria with  
513 neutral, positive, or negative responses (Balestra et al., 2011).

514 The taxonomic composition of PAB ( $>25 \mu\text{m}$ ) was substantially different from that of the bulk  
515 bacteria community in the hypoxic zone (with a large increase of  $\gamma$ -Pro associated with particles, Figure  
516 S2A). This result supports the previous report of  $\gamma$ -Pro being the most dominant clades attached to sinking  
517 particles in the ocean (DeLong et al., 1993). A broad range of species associated with  $\gamma$ -Pro was known to  
518 be important for quorum sensing processes due to their high population density (Doberva et al., 2015)  
519 associated with sinking or suspended aggregates (Krupke et al., 2016). In particular, the genus of  $\gamma$ -Pro such  
520 as *Alteromonas* and *Pseudomonas*, are well-known quorum-sensing bacteria that can rely on diverse  
521 signaling molecules to affect particle-associated bacterial communities by coordinating gene expression  
522 within the bacterial populations (Long et al., 2003; Fletcher et al., 2007).

523 It has been reported that the growths of some bacterial strains of the  $\gamma$ -Pro such as *Alteromonas* spp.  
524 and *Pseudomonas* spp. could be stimulated and regulated by oxylipins like PUAs (Ribalet et al., 2008; Pepi  
525 et al., 2017). Oxylipins were found to promote biofilm formation of *Pseudomonas* spp. (Martinez et al.,  
526 2016) and could serve as signaling molecules mediating cell-to-cell communication of *Pseudomonas* spp.  
527 by an oxylipin-dependent quorum sensing system (Martinez et al., 2019). As PUAs are an important group  
528 of chemical cues belonging to oxylipins (Franzè et al., 2018), it is thus reasonable to expect that PUAs may  
529 also participate as potential signaling molecules for the quorum sensing among a high-density *Alteromonas*  
530 or *Pseudomonas*. A high level of particle-adsorbed PUAs occurring on organic particles in the low-oxygen  
531 water would likely allow particle specialists such as *Alteromonas* to regulate bacterial community structure,

532 which could alter species richness and diversity of PAB as well as their metabolic functions such as  
533 respiration and production when interacting with particulate organic matter in the hypoxic zone. Various  
534 bacterial assemblages may have different rates and efficiencies of particulate organic matter degradation  
535 (Ebrahimi et al., 2019). Coordination amongst these PAB could be critical in their ability to thrive on the  
536 recycling of POC (Krupke et al., 2016) and thus likely contribute to the acceleration of oxygen utilizations  
537 in the hypoxic zone. Nevertheless, the molecular mechanism of the potential PUA-dependent quorum  
538 sensing of PAB may be an important topic for future study.

539 Our findings may likely apply to other coastal systems where there are large river inputs, intense  
540 phytoplankton blooms driven by eutrophication, and strong hypoxia, such as the Chesapeake Bay, the  
541 Adriatic Sea, and the Baltic Sea. For example, Chesapeake Bay is largely influenced by river runoff with  
542 strong eutrophication-driven hypoxia during the summer as a result of increased water stratification (Fennel  
543 and Testa, 2019) and enhanced microbial respiration fueled by organic carbons produced during spring  
544 diatom blooms (Harding et al., 2015). Similar to the PRE, there was also a high abundance of  $\gamma$ -Pro in the  
545 low-oxygen waters of the Chesapeake Bay associated with the respiration of resuspended organic carbon  
546 (Crump et al., 2007). Eutrophication causes intense phytoplankton blooms in the coastal ocean.  
547 Sedimentation of the phytoplankton carbons will lead to their accumulation in the surficial sediment  
548 (Cloern, 2001), including PUFA compounds derived from the lipid production. Resuspension and oxidation  
549 of these PUFA-rich organic particles during summer salt-wedge intrusion might lead to high  
550 particle-adsorbed PUAs in the water column. These PUAs could likely shift the particle-attached bacterial  
551 community to consume more oxygen when degrading particulate organic matter and thus potentially  
552 contribute to the formation of seasonal hypoxia. In this sense, the possible role of PUAs on coastal hypoxia  
553 may be a byproduct of eutrophication driven by anthropogenic nutrient loading. Further studies are required  
554 to quantify the contributions from PUAs-mediated oxygen loss by aerobic respiration to total  
555 deoxygenation in the coastal ocean.

556

## 557 **5. Conclusions**

558 In summary, we found elevated concentrations of pPUAs and dPUAs in the hypoxic waters below the  
559 salt-wedge. We also found high particle-adsorbed PUAs associated with particles of >25  $\mu\text{m}$  in the hypoxic  
560 waters based on the large-volume filtration method, which could generate a hotspot PUAs concentration  
561 of >10  $\mu\text{mol L}^{-1}$  in the water column. In the hypoxic waters, bacterial respiration was largely controlled by  
562 PAB (>0.8  $\mu\text{m}$ ) with FLB (0.2-0.8  $\mu\text{m}$ ) only accounting for 25-30% of the total respiration. Field  
563 PUA-amended experiments were conducted for PAB associated with particles of >25  $\mu\text{m}$  retrieved from the  
564 low-oxygen waters. We found distinct responses of PAB (>25  $\mu\text{m}$ ) to different doses of PUAs treatments  
565 with an increase of cell growth in response to low-dose PUAs (1  $\mu\text{mol L}^{-1}$ ) but an elevated cell-specific  
566 metabolic activity including bacterial respiration and production in response to high-dose PUAs (100  $\mu\text{mol}$   
567  $\text{L}^{-1}$ ). Improved cell-specific metabolism of PAB in response to high-dose PUAs was also accompanied by a  
568 substantial shift of bacterial community structure with increased dominance of genus *Alteromonas* within  
569 the  $\gamma$ -Pro.

570 Based on these observations, we hypothesize that PUAs may potentially act as signaling molecules for  
571 coordination among the high-density PAB below the salt-wedge, which would likely allow bacteria such as  
572 *Alteromonas* to thrive in degrading particulate organic matters. Very possibly, this process by changing  
573 community compositions and metabolic rates of PAB would lead to an increase of microbial oxygen  
574 utilization that might eventually contribute to the formation of coastal hypoxia.

575  
576 *Data availability.* Some of the data used in the present study are available in the Supplement. Other data  
577 analyzed in this article are tabulated herein. For any additional data please request from the corresponding  
578 author.

579  
580 *Supplement.* The supplement related to this article is available online at: [bg-2020-243-supplement](https://doi.org/10.1111/bg-2020-243-supplement).

581



582 *Author Contributions.* Q.P.L designed the project. Z.W. performed the experiments. Q.P.L and Z.W. wrote  
583 the paper with inputs from all co-authors. All authors have given approval to the final version of the  
584 manuscript.

585

586 *Competing interests.* The authors declare no competing financial interest.

587

588 *Acknowledgements.* We are grateful to the captains and the staff of *R/V Haike68* and *R/V Tan Kah Kee* for  
589 help during the cruises. We thank Profs Dongxiao Wang (SCSIO) and Xin Liu (XMU) for organizing the  
590 cruises, Mr. Yuchen Zhang (XMU) for field assistances, Profs Changsheng Zhang (SCSIO) and Weimin  
591 Zhang (GIM) for analytical assistance, as well as Prof. Dennis Hansell (RSMAS) for critical comments.

592

593 *Financial support.* This work was supported by the National Natural Science Foundation of China  
594 (41706181, 41676108), the National Key Research and Development Program of China  
595 (2016YFA0601203-02), and the Key Special Project for Introduced Talents Team of Southern Marine  
596 Science and Engineering Guangdong Laboratory (Guangzhou) (GML2019ZD0305). ZW also wants to  
597 acknowledge a visiting fellowship (MELRS1936) from the State of Key Laboratory of Marine  
598 Environmental Science (Xiamen University).

599 **REFERENCE**

- 600 Balestra, C., Alonso-Saez, L., Gasol, J. M., and Casotti, R.: Group-specific effects on coastal bacterioplankton of  
601 polyunsaturated aldehydes produced by diatoms, *Aquat. Microb. Ecol.*, 63, 123-131,  
602 <http://doi.org/10.3354/ame01486>, 2011.
- 603 Bartual, A., Morillo-Garcia, S., Ortega, M. J., and Cozar, A.: First report on vertical distribution of dissolved  
604 polyunsaturated aldehydes in marine coastal waters, *Mar. Chem.*, 204, 1-10.  
605 <https://doi.org/10.1016/j.marchem.2018.05.004>, 2018.
- 606 Breitburg, D., Levin, L. A., Oschlies, A., Gregoire, M., Chavez, F. P., Conley, D. J., Garcon, V., Gilbert, D., Gutierrez,  
607 D., Isensee, K., Jacinto, G. S., Limburg, K. E., Montes, I., Naqvi, S. W. A., Pitcher, G. C., Rabalais, N. N.,  
608 Roman, M. R., Rose, K. A., Seibel, B. A., Telszewski, M., Yasuhara, M., and Zhang, J.: Declining oxygen in the  
609 global ocean and coastal waters, *Science*, 359, eaam7240, <http://doi.org/10.1126/science.aam7240>, 2018.
- 610 Cloern, J. E.: Our evolving conceptual model of the coastal eutrophication problem, *Mar. Ecol. Prog. Ser.*, 210:  
611 223-253, <http://doi.org/10.3354/meps210223>, 2001.
- 612 Crump, B. C., Peranteau, C., Beckingham, B., and Cornwell J. C.: Respiratory succession and community succession  
613 of bacterioplankton in seasonally anoxic estuarine waters, *Appl. Environ. Microb.*, 73, 6802-6810,  
614 <http://doi.org/10.1128/aem.00648-07>, 2007.
- 615 Crump, B. C., Baross, J. A., and Simenstad, C. A.: Dominance of particle-attached bacteria in the Columbia River  
616 estuary, USA. *Aquat. Microb. Ecol.*, 14, 7-18, <http://doi.org/10.3354/ame014007>, 1998.
- 617 Decho, A.W., Visscher, P.T., Ferry, J., et al.: Autoinducers extracted from microbial mats reveal a surprising diversity  
618 of N-acylhomoserine lactones (AHLs) and abundance changes that may relate to diel pH. *Environ. Microb.*, 11:  
619 409-420, <https://doi.org/10.1111/j.1462-2920.2008.01780.x>, 2009
- 620 Delong, E. F., Franks, D. G., and Alldredge, A. L.: Phylogenetic diversity of aggregate-attached vs free-living marine  
621 bacterial assemblages, *Limnol. Oceanogr.* 38: 924-934, <http://doi.org/10.4319/lo.1993.38.5.0924>, 1993.
- 622 Diaz, R. J., and Rosenberg, R.: Spreading dead zones and consequences for marine ecosystems, *Science*, 321,  
623 926-929, <http://doi.org/10.1126/science.1156401>, 2008.
- 624 Doberva, M., Sanchez-Ferandin, S., Toulza, E., Lebaron P., and Lami, R.: Diversity of quorum sensing autoinducer  
625 synthases in the Global Ocean Sampling metagenomic database, *Aquat. Microb. Ecol.* 74: 107-119,  
626 <http://doi.org/10.3354/ame01734>, 2015.
- 627 Doney, S. C., Ruckelshaus, M., Duffy, J. E., Barry, J. P., Chan, F., English, C. A., Galindo, H. M., Grebmeier, J. M.,  
628 Hollowed, A. B., Knowlton, N., Polovina, J., Rabalais, N. N., Sydeman, W. J., and Talley, L. D.: Climate change  
629 impacts on marine ecosystems, *Annu. Rev. Mar. Sci.*, 4, 11-37,  
630 <http://doi.org/10.1146/annurev-marine-041911-111611>, 2012.
- 631 Dyksterhouse, S. E., Gray J. P., Herwig R. P., Lara J. C. and Staley J. T.: *Cycloclasticus pugetii* gen. nov., sp. nov., an  
632 aromatic hydrocarbon-degrading bacterium from marine sediments, *Int. J. of Syst. Bacteriol.*, 45: 116-123,  
633 <http://doi.org/10.1099/00207713-45-1-116>, 1995.
- 634 Edwards, B. R., Bidle, K. D., and van Mooy, B. A. S.: Dose-dependent regulation of microbial activity on sinking

635 particles by polyunsaturated aldehydes: implications for the carbon cycle, *P. Natl. Acad. Sci. USA.*, 112,  
636 5909-5914, <http://doi.org/10.1073/pnas.1422664112>, 2015.

637 Ebrahimi, A., Schwartzman, J., and Cordero, O. X.: Cooperation and self-organization determine rate and efficiency  
638 of particulate organic matter degradation in marine bacteria, *P. Natl. Acad. Sci. USA.*, 116, 23309-23316,  
639 <http://doi.org/10.1073/pnas.1908512116>, 2019.

640 Fennel, K., and Testa, J. M.: Biogeochemical Controls on Coastal Hypoxia, *Annu. Rev. Mar. Sci.*, 11, 4.1-4.26,  
641 <http://doi.org/10.1146/annurev-marine-010318-095138>, 2019.

642 Fletcher, M. P., Diggle, S. P., Crusz, S. A., Chhabra, S. R., Camara, M., and Williams, P.: A dual biosensor for  
643 2-alkyl-4-quinolone quorum-sensing signal molecules, *Environ. Microbiol.*, 9: 2683-2693,  
644 <http://doi.org/10.1111/j.1462-2920.2007.01380.x>, 2007.

645 Franzè, G., Pierson, J. J., Stoecker, D. K., and Lavrentyev, P. J.: Diatom-produced allelochemicals trigger trophic  
646 cascades in the planktonic food web, *Limnol. Oceanogr.*, 63, 1093-1108, <http://doi.org/10.1002/lno.10756>, 2018.

647 Fuchsman, C.A., Kirkpatrick, J.B., Brazelton, W.J., Murray, J.W., and Staley, J.T.: Metabolic strategies of free-living  
648 and aggregate-associated bacterial communities inferred from biologic and chemical profiles in the Black Sea  
649 suboxic zone. *FEMS Microbiol Ecol*, 78: 586-603. <https://doi.org/10.1111/j.1574-6941.2011.01189.x>, 2011.

650 Galeron, M. A., Radakovitch, O., Charriere, B., Vaultier, F., Volkman, J. K., Bianchi, T. S., Ward, N. D., Medeiros, P.  
651 M., Sawakuchi, H. O., Tank, S., Kerherve, P., and Rontani, J. F.: Lipoxxygenase-induced autoxidative degradation  
652 of terrestrial particulate organic matter in estuaries: A widespread process enhanced at high and low latitude, *Org.*  
653 *Geochem.*, 115, 78-92, <http://doi.org/10.1016/j.orggeochem.2017.10.013>, 2018.

654 García-Martín, E. E., Aranguren-Gassis, M., Karl, D. M., et al.: Validation of the in vivo Iodo-Nitro-Tetrazolium  
655 (INT) salt reduction method as a proxy for plankton respiration. *Front. Mar. Sci.*, 6, 220,  
656 <http://doi.org/10.3389/fmars.2019.00220>, 2019

657 Garneau, M.E., Vincent, W.F., Terrado, R., and Lovejoy, C.: Importance of particle-associated bacterial heterotrophy  
658 in a coastal Arctic ecosystem, *J. Marine Syst.*, 75, 185-197, <http://doi.org/10.1016/j.jmarsys.2008.09.002>, 2009.

659 Ge, Z., Wu, Z., Liu Z., Zhou, W., Dong, Y., and Li, Q. P.: Using detaching method to determine the abundance of  
660 particle-attached bacteria from the Pearl River Estuary and its coupling relationship with environmental factors,  
661 *Chinese J. Mar. Environ. Sci.*, <http://doi.org/10.12111/j.mes.20190065>, 2020.

662 Harding, Jr. L. W., , Adolf, J. E., Mallonee, M. E., Miller, W. D., Gallegos, C. L., Perry, E. S., Johnson, J. M., Sellner,  
663 K. G., and Paerl H. W.: Climate effects on phytoplankton floral composition in Chesapeake Bay, *Estuar. Coast.*  
664 *Shelf S.*, 162, 53-68, <http://doi.org/10.1016/j.ecss.2014.12.030>, 2015.

665 He, B. Dai, M., Zhai, W., Guo, X., and Wang, L.: Hypoxia in the upper reaches of the Pearl River Estuary and its  
666 maintenance mechanisms: A synthesis based on multiple year observations during 2000-2008, *Mar. Chem.*, 167,  
667 13-24, <http://doi.org/10.1016/j.marchem.2014.07.003>, 2014.

668 Hopkinson, C.S.: Shallow-water benthic and pelagic metabolism- evidence of heterotrophy in the nearshore Georgia  
669 bight, *Mar. Biol.*, 87, 19-32, <http://doi.org/10.1007/bf00397002>, 1985.

670 Helm, K. P., Bindoff, N. L., and Church, J. A.: Observed decreases in oxygen content of the global ocean, *Geophys.*

671 Res. Lett., 38, L23602. <http://doi.org/10.1029/2011GL049513>, 2011.

672 Hmelo, L. R., Mincer, T. J., and Van Mooy, B. A. S.: Possible influence of bacterial quorum sensing on the hydrolysis  
673 of sinking particulate organic carbon in marine environments, *Env. Microbiol. Rep.*, 3, 682-688,  
674 <http://doi.org/10.1111/j.1758-2229.2011.00281.x>, 2011.

675 Huang, Y., Liu, X., Laws, E. A., Chen, B., Li, Y., Xie, Y., Wu, Y., Gao, K., and Huang, B.: Effects of increasing  
676 atmospheric CO<sub>2</sub> on the marine phytoplankton and bacterial metabolism during a bloom: A coastal mesocosm  
677 study, *Sci. Total Environ.*, 633, 618-629, <http://doi.org/10.1016/j.scitotenv.2018.03.222>, 2018.

678 Hu, J., Zhang H., and Peng P.: Fatty acid composition of surface sediments in the subtropical Pearl River estuary and  
679 adjacent shelf, Southern China. *Estuar. Coast, Shelf S.*, 66: 346-356, <http://doi.org/10.1016/j.ecss.2005.09.009>,  
680 2006.

681 Ianora, A., and Miralto, A.: Toxicogenic effects of diatoms on grazers, phytoplankton and other microbes: a review,  
682 *Ecotoxicology*, 19, 493-511, <http://doi.org/10.1007/s10646-009-0434-y>, 2010.

683 Ivars-Martinez, E., Martin-Cuadrado, A. B., D'Auria, G., Mira, A., Ferriera, S., Johnson, J., et al.: Comparative  
684 genomics of two ecotypes of the marine planktonic copiotroph *Alteromonas macleodii* suggests alternative  
685 lifestyles associated with different kinds of particulate organic matter. *ISME, J2*, 1194–1212, 2008.

686 Kemp, W. M., Testa, J. M., Conley, D. J., Gilbert, D., and Hagy, J. D.: Temporal responses of coastal hypoxia to  
687 nutrient loading and physical controls, *Biogeosciences*, 6, 2985-3008, <http://doi.org/10.5194/bg-6-2985-2009>,  
688 2009.

689 Krupke, A., Hmelo, L. R., Ossolinski, J. E., Mincer, T. J., and Van Mooy, B. A. S.: Quorum sensing plays a complex  
690 role in regulating the enzyme hydrolysis activity of microbes associated with sinking particles in the ocean,  
691 *Front. Mar. Sci.*, 3:55, <http://doi.org/10.3389/fmars.2016.00055>, 2016.

692 Kirchman D. L.: Leucine incorporation as a measure of biomass production by heterotrophic bacteria, in: *Hand book*  
693 *of methods in aquatic microbial ecology*, edited by: Kemp, P. F., Cole, J. J., Sherr, B. F., and Sherr, E. B., Lewis  
694 Publishers, Boca Raton, 509–512, <http://doi.org/10.1201/9780203752746-59>, 1993.

695 Kirchman D. L.: *Microbial ecology of the oceans*, 2nd Ed., Hoboken, New Jersey, Wiley, 1-593,  
696 <http://doi.org/10.1002/9780470281840>, 2008.

697 Lee, S., Lee, C., Bong, C., Narayanan, K., and Sim, E.: The dynamics of attached and free-living bacterial population  
698 in tropical coastal waters, *Mar. Freshwater Res.*, 66, 701-710, <http://doi.org/10.1071/mf14123>, 2015.

699 Li, J., Salam, N., Wang, P. et al.: Discordance between resident and active bacterioplankton in free-living and  
700 particle-associated communities in estuary ecosystem. *Microb. Ecol.*, 76, 637–647,  
701 <https://doi.org/10.1007/s00248-018-1174-4>, 2018

702 Liu, Y., Lin, Q., Feng, J., et al.: Differences in metabolic potential between particle-associated and free-living  
703 bacteria along Pearl River Estuary, *Sci. Total Environ.*, 728, 138856,  
704 <https://doi.org/10.1016/j.scitotenv.2020.138856>, 2020

705 Long, R. A., Qureshi, A., Faulkner, D. J., and Azam, F.: 2-n-pentyl-4-quinolinol produced by a marine *Alteromonas*  
706 sp and its potential ecological and biogeochemical roles, *Appl. Environ. Microb.*, 69, 568-576,

707 <http://doi.org/10.1128/aem.69.1.568-576.2003>, 2003.

708 Lu, Z., Gan, J., Dai, M., Liu, H., and Zhao, X.: Joint effects of extrinsic biophysical fluxes and intrinsic  
709 hydrodynamics on the formation of hypoxia west off the Pearl River Estuary, *J. Geophys. Res.-Oceans.*, 123,  
710 <https://doi.org/10.1029/2018JC014199>, 2018.

711 Lunau, M., Lemke, A., Walther, K., Martens-Habbena, W., and Simon, M.: An improved method for counting  
712 bacteria from sediments and turbid environments by epifluorescence microscopy, *Environ. Microbiol.*, 7,  
713 961-968, <http://doi.org/10.1111/j.1462-2920.2005.00767.x>, 2005.

714 Marie, D., Partensky, F., Jacquet, S. and Vaulot, D.: Enumeration and cell cycle analysis of natural populations of  
715 marine picoplankton by flow cytometry using the nucleic acid stain SYBR Green I, *Appl. Environ. Microbiol.*,  
716 63, 186-193, <http://doi.org/10.1128/AEM.63.1.186-193.1997>, 1997.

717 Martinez, E., and Campos-Gomez, J.: Oxylipins produced by *Pseudomonas aeruginosa* promote biofilm formation  
718 and virulence, *Nat. Commun.*, 7, 13823, <https://doi.org/10.1038/ncomms13823>, 2016.

719 Martinez, E., Cosnahan, R. K., Wu, M. S., Gadila, S. K., Quick, E. B., Mobley, J. A., and Campos-Gomez, J.:  
720 Oxylipins mediate cell-to-cell communication in *Pseudomonas aeruginosa*, *Commun. Biol.*, 2, 66,  
721 <https://doi.org/10.1038/s42003-019-0310-0>, 2019.

722 Mestre, M., Borrull, E., Sala, M., et al.: Patterns of bacterial diversity in the marine planktonic particulate matter  
723 continuum, *ISME J.*, 11, 999-1010, <https://doi.org/10.1038/ismej.2016.166>, 2017.

724 Oudot, C., Gerard, R., Morin, P., and Gningue, I.: Precise shipboard determination of dissolved-oxygen (winkler  
725 procedure) for productivity studies with a commercial system, *Limnol. Oceanogr.*, 33, 146-150,  
726 <http://doi.org/10.4319/lo.1988.33.1.0146>, 1988.

727 Parsons, T. R., Maita, Y., and Lalli, C. M.: Fluorometric Determination of Chlorophylls, in: *A manual of chemical*  
728 *and biological methods for seawater analysis*, Pergamum Press, Oxford, 107-109,  
729 <http://doi.org/10.1016/B978-0-08-030287-4.50034-7>, 1984.

730 Paul, C., Reunamo, A., Lindehoff, E., et al.: Diatom derived polyunsaturated aldehydes do not structure the  
731 planktonic microbial community in a mesocosm study, *Mar. Drugs*, 10, 775-792,  
732 <http://doi.org/10.3390/md10040775>, 2012.

733 Pepi, M., Heipieper, H. J., Balestra, C., Borra, M., Biffali, E., and Casotti, R.: Toxicity of diatom polyunsaturated  
734 aldehydes to marine bacterial isolates reveals their mode of action, *Chemosphere*, 177, 258-265, 2017

735 Ploug, H., Zimmermann-Timm, H., and Schweitzer, B.: Microbial communities and respiration on aggregates in the  
736 Elbe Estuary, Germany, *Aquat. Microb. Ecol.*, 27:241-248, 2002

737 Pohnert, G.: Wound-activated chemical defense in unicellular planktonic algae, *Ange. Chem. Int. Edit.*, 39,  
738 4352-4354. [https://doi.org/10.1002/1521-3773\(20001201\)39:23<4352::AID-ANIE4352>3.0.CO;2-U](https://doi.org/10.1002/1521-3773(20001201)39:23<4352::AID-ANIE4352>3.0.CO;2-U), 2000

739 Rabouille, C., Conley, D. J., Dai, M. H., Cai, W. J., Chen, C. T. A., Lansard, B., Green, R., Yin, K., Harrison, P. J.,  
740 Dagg, M., and McKee, B.: Comparison of hypoxia among four river-dominated ocean margins: The Changjiang  
741 (Yangtze), Mississippi, Pearl, and Rhone rivers, *Cont. Shelf Res.*, 28, 1527-1537,  
742 <http://doi.org/10.1016/j.csr.2008.01.020>, 2008.

743 Ribalet, F., Intertaglia, L., Lebaron, P., and Casotti, R.: Differential effect of three polyunsaturated aldehydes on  
744 marine bacterial isolates, *Aquat. Toxicol.*, 86, 249-255, <http://doi.org/10.1016/j.aquatox.2007.11.005>, 2008.

745 Rink, B., Lunau, M., Seeberger, S., et al.: Diversity patterns of aggregate-associated and free-living bacterial  
746 communities in the German Wadden Sea, *Ber Forschungszentrum Terramare*, 12: 96–98, 2003.

747 Robinson, C., and Williams, P. J. I.: Respiration and its measurement in surface marine waters, in: *Respiration in*  
748 *Aquatic Ecosystems*, edited by de Giorgio, P. A., and Williams, P. J. I., Oxford University Press, New York,  
749 147-180, <http://doi.org/10.1093/acprof:oso/9780198527084.003.0009>, 2005.

750 Su, J., Dai, M., He, B., Wang, L., Gan, J., Guo, X., Zhao, H., and Yu, F.: Tracing the origin of the oxygen-consuming  
751 organic matter in the hypoxic zone in a large eutrophic estuary: the lower reach of the Pearl River Estuary, China,  
752 *Biogeosciences*, 14, 4085-4099, <http://doi.org/10.5194/bg-14-4085-2017>, 2017.

753 Vidoudez, C., Casotti, R., Bastianini, M., and Pohnert, G.: Quantification of dissolved and particulate polyunsaturated  
754 aldehydes in the Adriatic Sea. *Mar. Drugs*, 9, 500-513, <https://doi.org/10.3390/md9040500>, 2011.

755 Wang, N., Lin, W., Chen, B., and Huang, B.: Metabolic states of the Taiwan Strait and the northern South China Sea  
756 in summer 2012, *J. Trop. Oceanogr.*, 33, 61-68, <http://doi.org/doi:10.3969/j.issn.1009-5470.2014.04.008>, 2014.

757 Williams, P. J. I. and de Giorgio, P. A.: Respiration in Aquatic Ecosystems: history and background, in: *Respiration in*  
758 *Aquatic Ecosystems*, edited by de Giorgio, P. A., and Williams, P. J. I., Oxford University Press, New York, 1-17,  
759 <http://doi.org/10.1093/acprof:oso/9780198527084.003.0001>, 2005.

760 Wu, Z., and Li, Q. P.: Spatial distributions of polyunsaturated aldehydes and their biogeochemical implications in the  
761 Pearl River Estuary and the adjacent northern South China Sea, *Prog. Oceanogr.*, 147, 1-9,  
762 <http://doi.org/10.1016/j.pocean.2016.07.010>, 2016.

763 Xu, J., Li, X., Shi, Z., Li, R., and Li, Q. P.: Bacterial carbon cycling in the river plume in the northern South China  
764 Sea during summer, *J. Geophys. Res.-Oceans*, 123, 8106-8121, <http://doi.org/10.1029/2018jc014277>, 2018.

765 Yin, K., Lin, Z., and Ke, Z.: Temporal and spatial distribution of dissolved oxygen in the Pearl River Estuary and  
766 adjacent coastal waters, *Cont. Shelf Res.*, 24, 1935-1948, <http://doi.org/10.1016/j.csr.2004.06.017>, 2004.

767 Zhang, H., and Li, S.: Effects of physical and biochemical processes on the dissolved oxygen budget for the Pearl  
768 River Estuary during summer, *J. Marine Syst.*, 79, 65-88, <http://doi.org/10.1016/j.jmarsys.2009.07.002>, 2010.

769 Zhang, Y., Xiao, W., and Jiao, N.: Linking biochemical properties of particles to particle-attached and free-living  
770 bacterial community structure along the particle density gradient from freshwater to open ocean, *J. Geophys.*  
771 *Res.-Bioge.*, 121, 2261-2274, <http://doi.org/10.1002/2016jg003390>, 2016.

772 **Table 1.** Summary of treatments in the experiments of exogenous PUAs additions for the low-oxygen  
773 waters at station Y1 during June 2019. The PUAs solution includes heptadienal (C7\_PUA), octadienal  
774 (C8\_PUA), and decadienal (C10\_PUA) with the mole ratios of 10:1:10.  
775

		<b>Treatment</b>
1	Control (methanol)	methanol
2	Low-dose PUAs (methanol)	2 mM PUAs in methanol
3	High-dose PUAs (methanol)	200 mM PUAs in methanol

776  
777

## Figures and Legends

778

779 **Figure 1:** Sampling map of the Pearl River Estuary and the adjacent northern South China Sea during (A)  
780 June 17<sup>th</sup>-28<sup>th</sup>, 2016, (B) June 18<sup>st</sup>-June 2<sup>nd</sup>, 2019. Contour shows the bottom oxygen distribution with  
781 white lines highlighting the levels of 93.5  $\mu\text{mol kg}^{-1}$  (oxygen-deficient zone) and 62.5  $\mu\text{mol kg}^{-1}$  (hypoxic  
782 zone); dashed line in panel A is an estuary-to-shelf transect with blue dots for three stations with bacterial  
783 metabolic rate measurements; diamonds in panel B are two stations with vertical pPUAs and dPUAs  
784 measurements with Y1 the station for PUAs-amended experiments.

785

786 **Figure 2:** Procedure of large-volume filtration and subsequent experiments. A large volume of the  
787 low-oxygen water was filtered through a 25- $\mu\text{m}$  filter to obtain the particles-adsorbed PUAs and the  
788 particle-attached bacteria (PAB). The carbon-source test of PUA for the inoculated PAB includes the  
789 additions of PUA, alkanes (ALK), and polycyclic aromatic hydrocarbons (PAH). PUAs-amended  
790 experiments for PAB include Control (CT), Low-dose (PL), and High-dose PUAs (PH). Samples in the  
791 biological oxygen demand (BOD) bottles at the end of the experiment were analysed for bacterial  
792 respiration (BR), abundances (BA), production (BP) as well as DNA. Note that pPUAs and dPUAs are  
793 particulate and dissolved PUAs in the seawater.

794

795 **Figure 3:** Vertical distributions of (A) temperature, (B) turbidity, (C) nitrate, (D) salinity, (E) dissolved  
796 oxygen, and (F) chlorophyll-*a* from the estuary to the shelf of the NSCS during June 2016. Section  
797 locations are shown in Figure 1; the white line in panel D shows the area of oxygen deficiency zone (<93.5  
798  $\mu\text{mol kg}^{-1}$ ).

799

800 **Figure 4:** Comparisons of oxygen, bulk bacterial respiration (BR) and production (BP), as well as bulk  
801 bacterial abundances (BA) of  $\alpha$ -Proteobacteria ( $\alpha$ -Pro),  $\gamma$ -Proteobacteria ( $\gamma$ -Pro), Bacteroidetes (Bact), and  
802 other bacteria for the bottom waters between stations inside (X1) and outside (X2 and X3) the hypoxic zone  
803 during the 2016 cruise. Bulk bacteria community includes FLB and PAB of <20  $\mu\text{m}$ . Locations of stations  
804 X1, X2, X3 are showed in Figure 1A. Error bars are the standard deviations.

805

806 **Figure 5:** Vertical distributions of (A) temperature, (B) salinity, (C) dissolved oxygen (DO), (D)  
807 chlorophyll-*a* (Chl-*a*), (E) particulate PUAs (pPUAs) and (F) dissolved PUAs (dPUAs) inside (Y1) and  
808 outside (Y2) the hypoxic zone during June 2019. Locations of station Y1 and Y2 are shown in Figure 1.  
809 Error bars are the standard deviations.

810

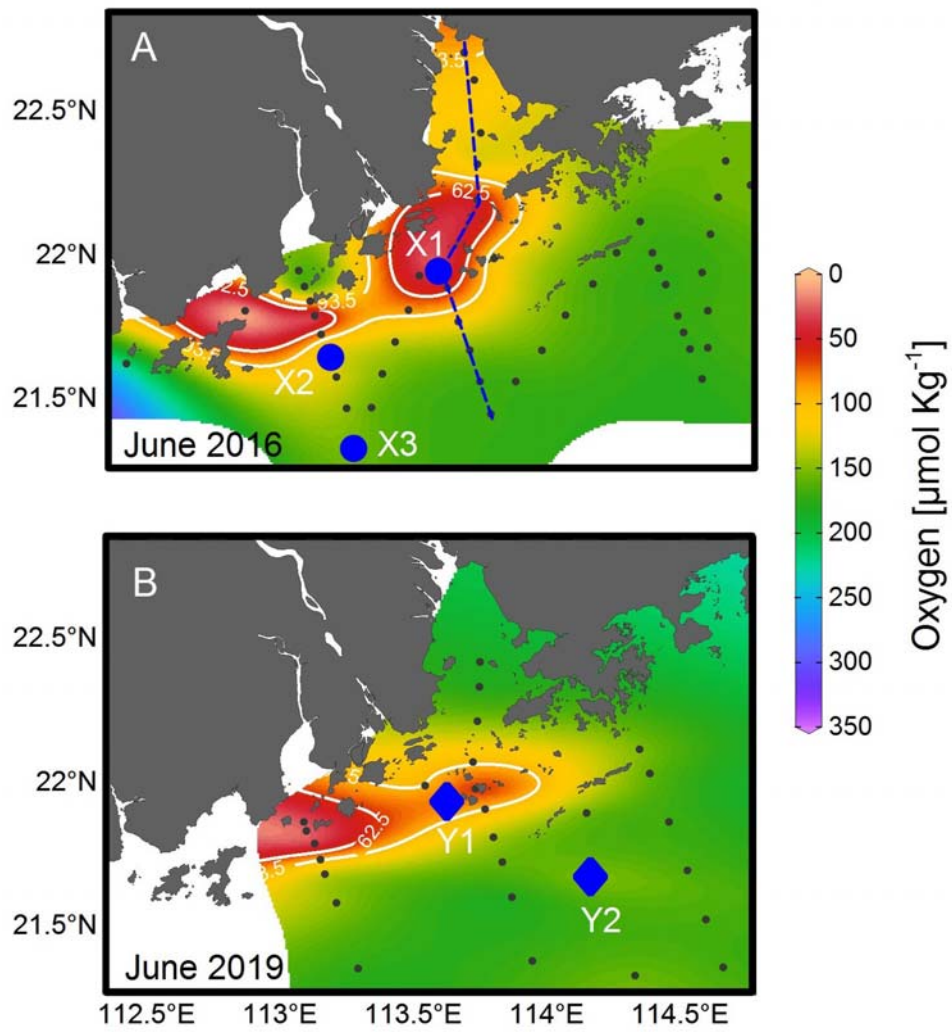


811 **Figure 6:** Concentrations of particle-adsorbed PUAs (in micromoles per liter particle) in the middle (12 m)  
812 and the bottom (25 m) waters of station Y1 during June 2019. Three different PUA components are also  
813 shown including heptadienal (C7\_PUA), octadienal (C8\_PUA), and decadienal (C10\_PUA). Error bars are  
814 the standard deviations.

815  
816 **Figure 7:** Responses of particle-attached bacterial parameters including (A) bacterial abundance ( $BA_{\text{particle}}$ ),  
817 (B) bacterial respiration ( $BR_{\text{particle}}$ ), (C) cell-specific bacterial respiration ( $sBR_{\text{particle}}$ ), (D) bacterial growth  
818 efficiency ( $BGE_{\text{particle}}$ ), (E) bacterial production ( $BP_{\text{particle}}$ ), and (F) cell-specific bacterial production  
819 ( $sBP_{\text{particle}}$ ) to different doses of PUAs additions at the end of the experiments for the middle (12 m) and the  
820 bottom waters (25 m) at station Y1. Error bars are standard deviations. The star represents a significant  
821 difference ( $p < 0.05$ ) with PL and PH the low and high dose PUA treatments and C the control.

822  
823 **Figure 8:** Variation of particle-attached bacterial community compositions on (A) the phylum level and (B)  
824 the genus level in response to different doses of PUAs additions at the end of the experiments for the  
825 middle and the bottom waters at station Y1. Labels PL and PH are for the low- and high-dose PUAs with  
826 CT the control.

827  
828 **Figure 9:** Carbon-source test of PUAs with cell culture of particle-attached bacteria inoculated from the  
829 low-oxygen waters of station Y1 including the initial conditions (Day0) at the beginning of the experiments  
830 as well as results after 30 days of incubations (Day30) for (A, B) the middle and (C, D) the bottom waters,  
831 respectively. Bottles from left to right are the mediums (M) with the additions of polycyclic aromatic  
832 hydrocarbons (M+PAH, 200 ppm), alkanes (M+ALK,  $0.25 \text{ g L}^{-1}$ ), and heptadienal (M+C7\_PUA,  $0.2 \text{ mmol}$   
833  $\text{L}^{-1}$ ); Note that a change of turbidity should indicate bacterial utilization of organic carbons. (E) the optical  
834 density of bacterium *Alteromonas hispanica* MOLA151 growing in the minimal medium as well as in the  
835 mediums with the additions of mannitol, pyruvate, and proline (M+MPP, 1% each), heptadienal  
836 (M+C7\_PUA,  $145 \mu\text{M}$ ), octadienal (M+C8\_PUA,  $130 \mu\text{M}$ ), and decadienal (M+C10\_PUA,  $106 \mu\text{M}$ ). The  
837 method for *A. hispanica* growth and the data in panel E are from Ribalet et al., 2008.



839

840

841

842

**Figure 1**

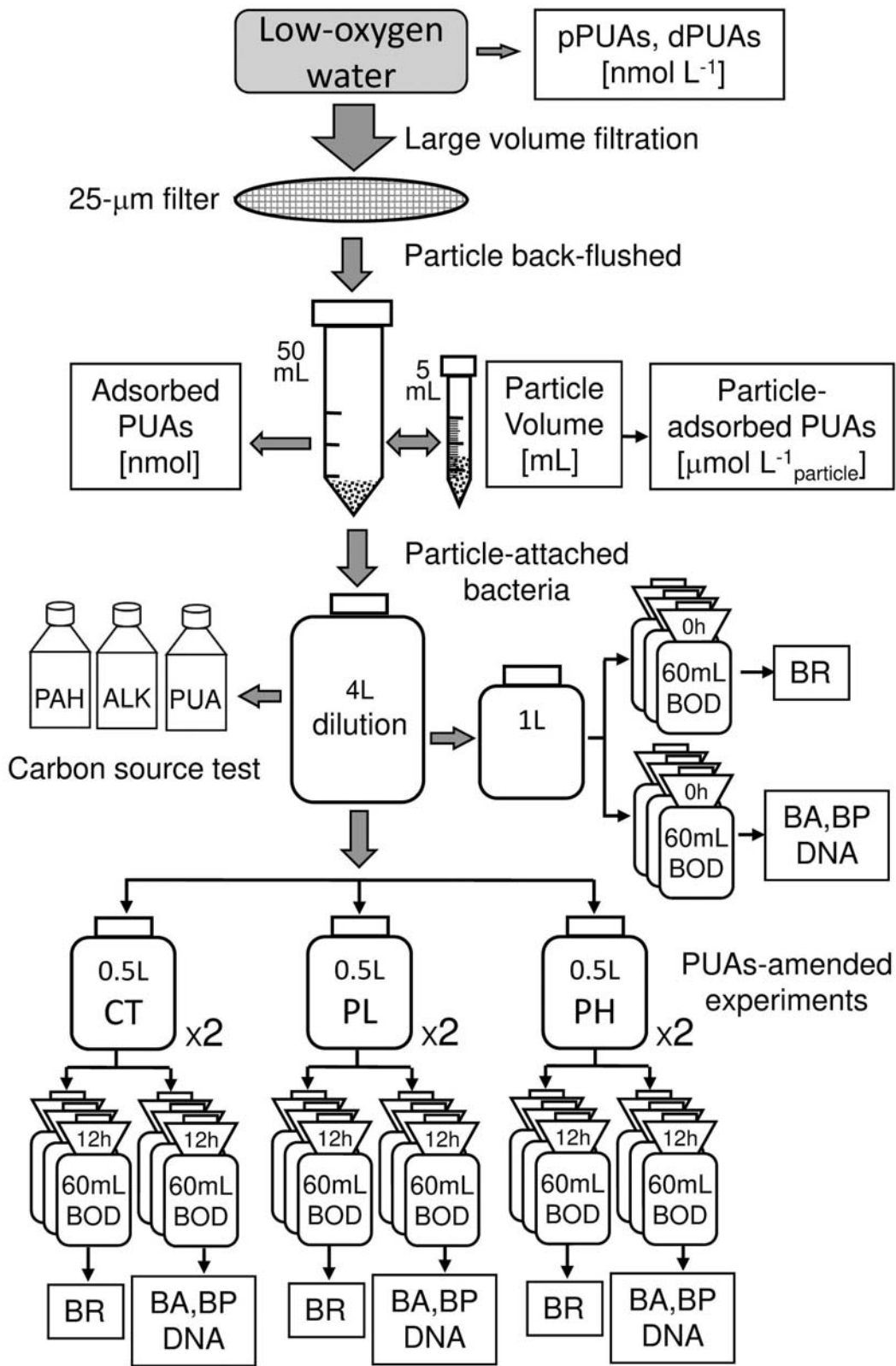
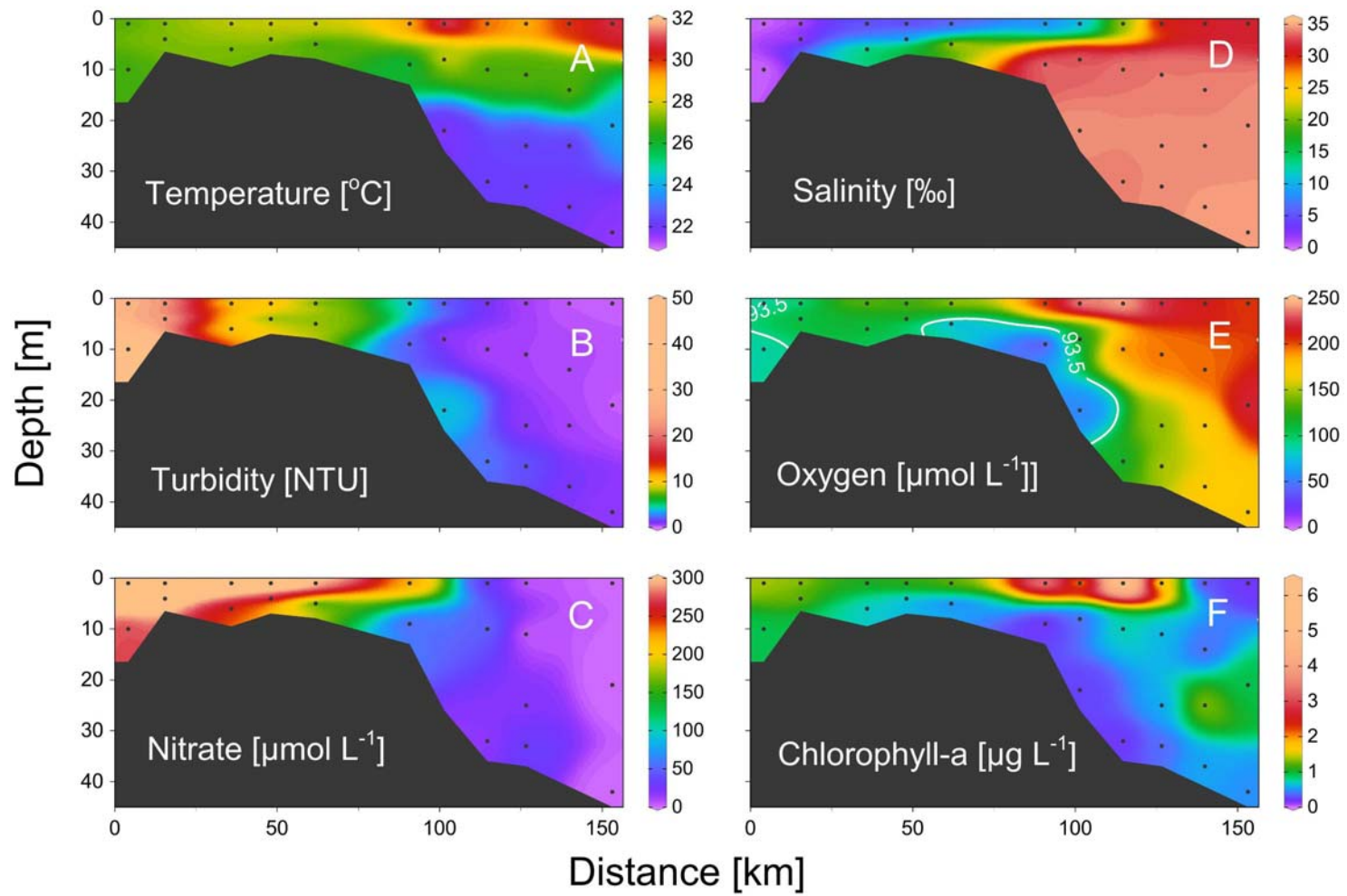


Figure 2

843

844

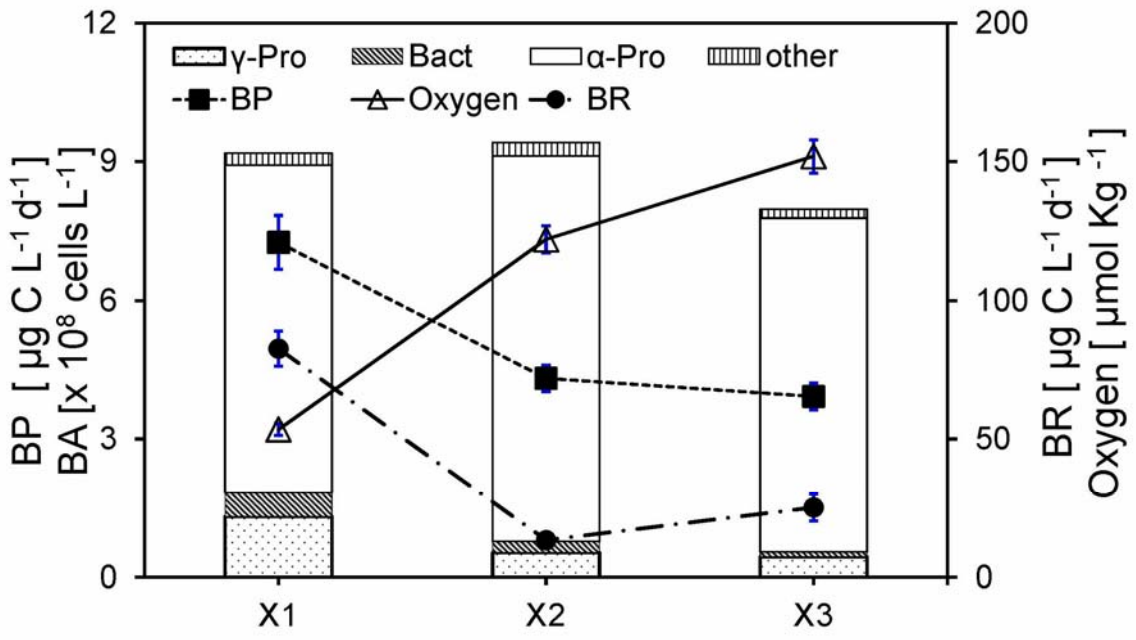


845

846

847

**Figure 3**



848  
849  
850  
851

Figure 4

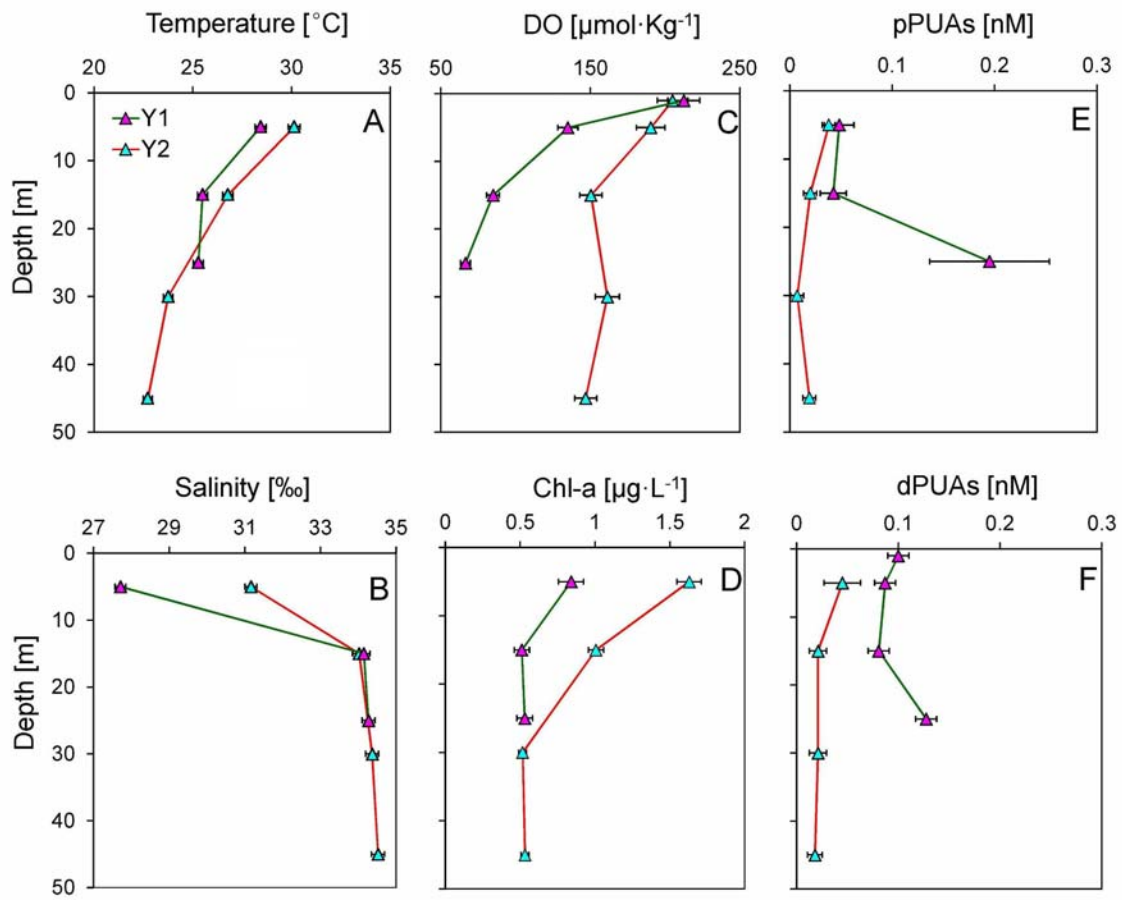


Figure 5

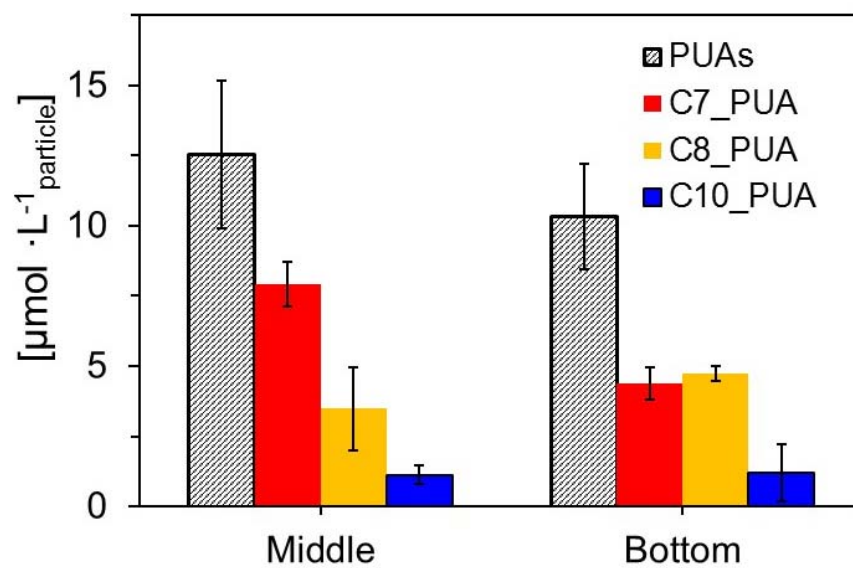
852

853

854

855

### Particle adsorbed PUAs



856  
857  
858  
859

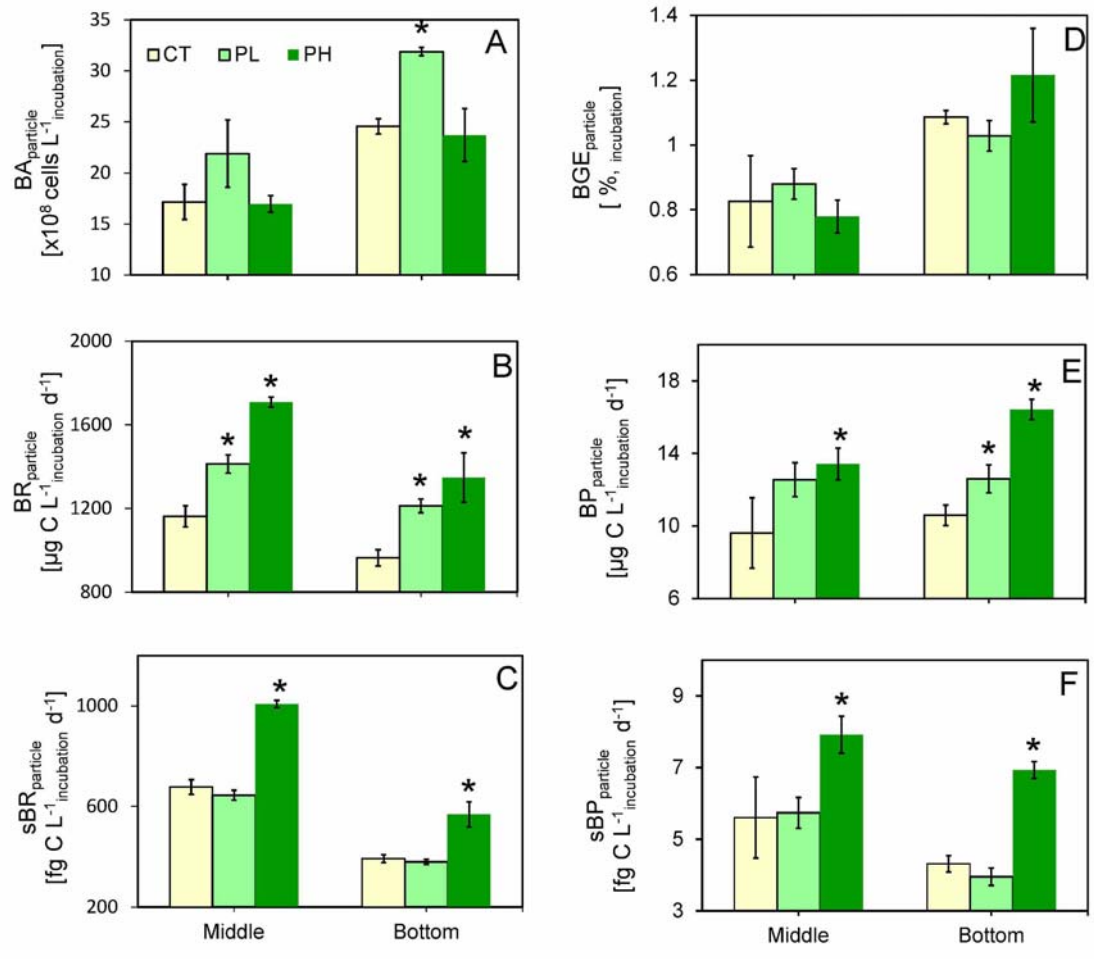


Figure 7

860  
861  
862  
863



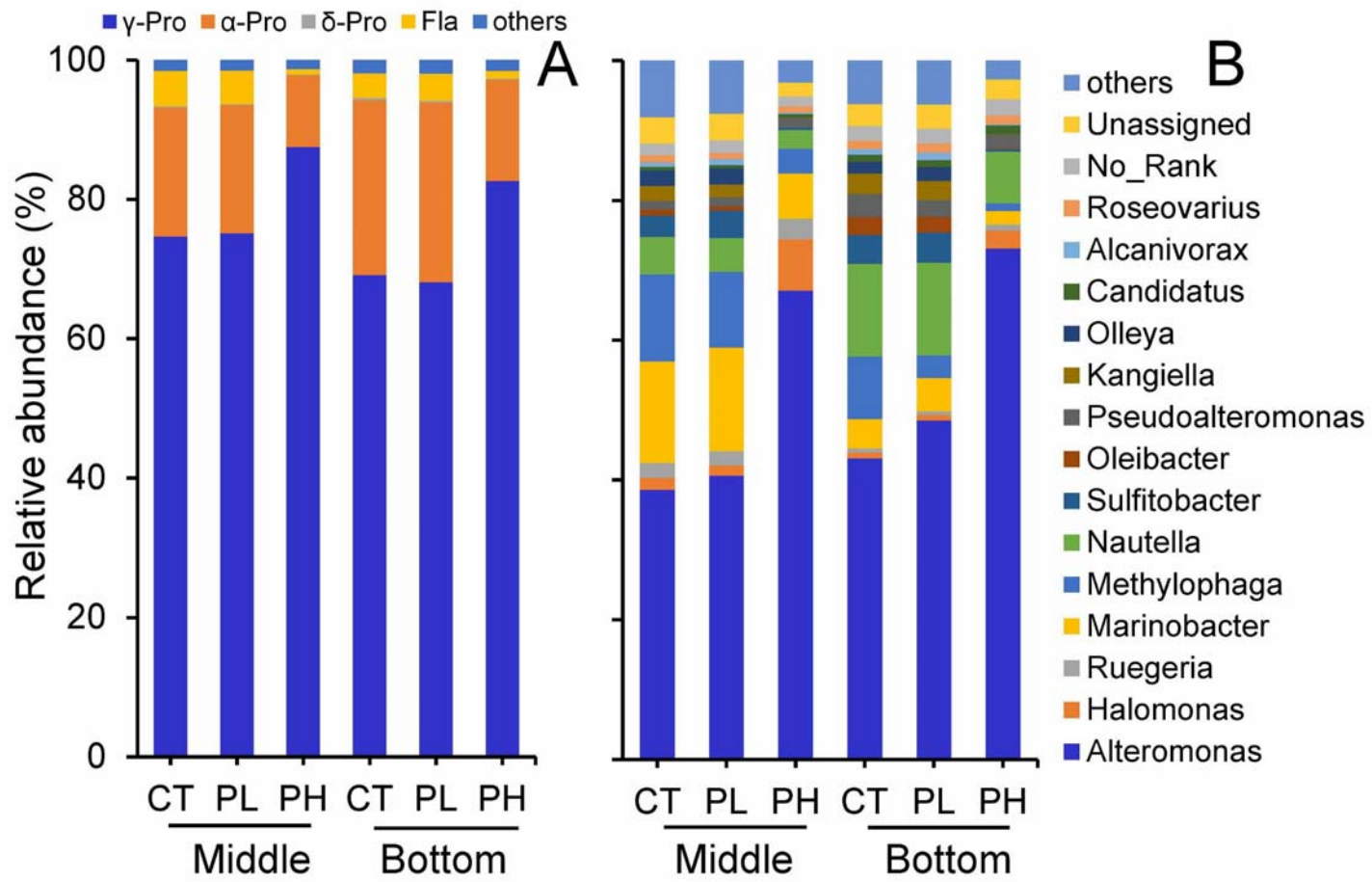


Figure 8

864

865

866

867  
868  
869  
870

